MASTERS PROJECT

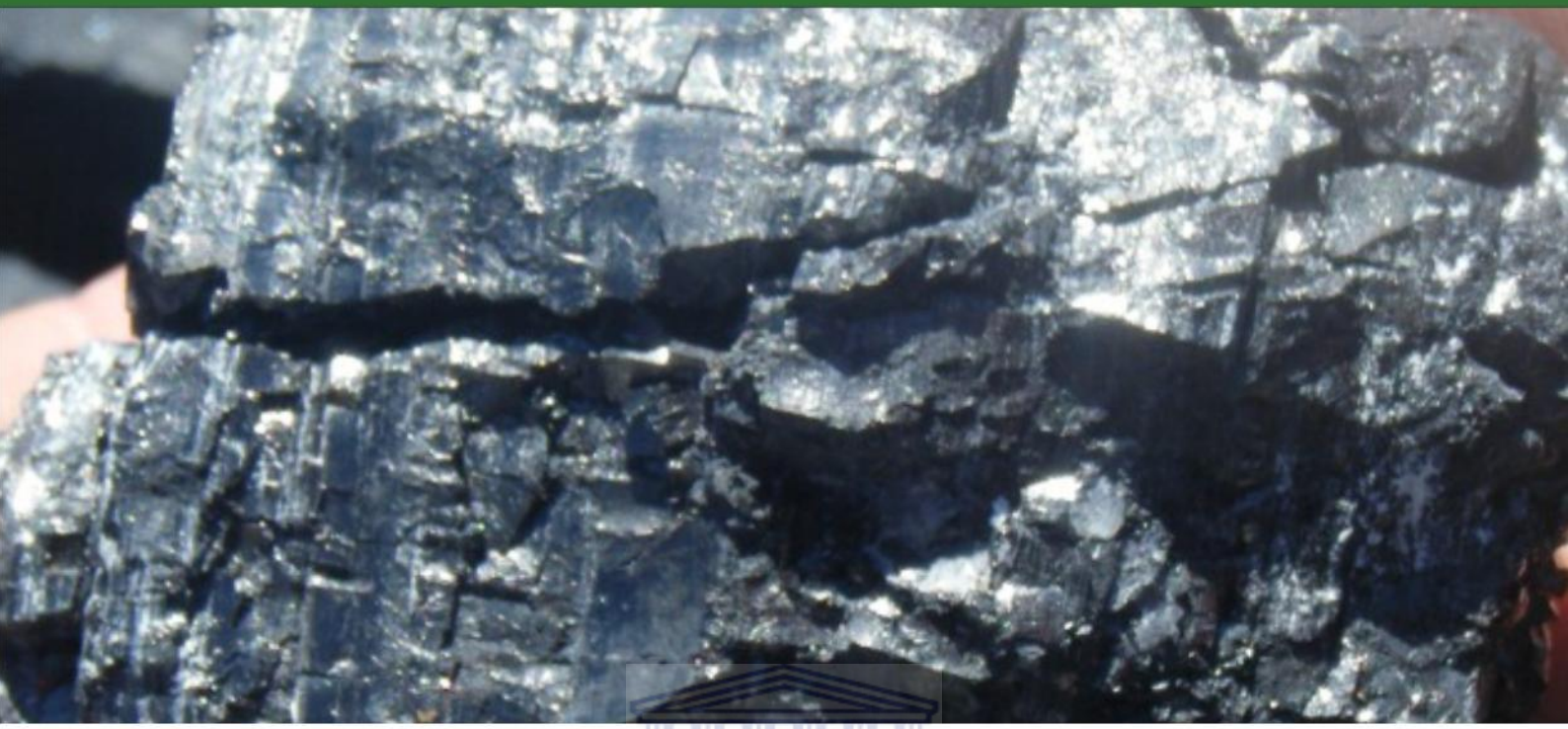

REGIONAL STRUCTURE OF THE CENTRAL KALAHARI SUB-BASIN AND THE GEOMETRY AND EFFECT OF THE DOLERITE SILLS IN THE AREA

Prepared by:
Leilah Gharbaharan

Supervisor: Dr. Russel Bailie
Co-supervisor: Prof. David Reid (UCT)
Advisor: Junior Potgieter

Prepared for:

sasol
reaching new frontiers

UNIVERSITY of the WESTERN CAPE

This is a Masters Project for partial fulfilment of the requirements of the Master of Science degree in Petroleum Geology at the University of the Western Cape.

2014

PLAGIARISM DECLARATION

I know that plagiarism is wrong. Plagiarism is to use another's work and pretend that it is one's own. Each significant contribution to, and quotation in this thesis from the work of other people has been attributed and has been cited and referenced. I have not allowed, and will not allow anyone to copy my work with the intention of passing it off as his or her own work.

Signature: _____

Date: _____

Abstract

The potential for Coal Bed Methane (CBM) has been assessed in the Karoo-aged coal seams in Eastern Botswana. This region is underlain by the Central Kalahari sub-basin of the Karoo Sequence and hosts a major thermal coal producer in the Morupule Mine. Coal bearing strata at depth in the sub-basin that are thought to be a source of CBM, occurs over an area bounded by the Okavango Dyke Swarm to the north, the Zoetfontein Fault to the south and the Kalahari Line to the west. The basin terminates to the east as a pinch out, with Karoo strata outcropping at the surface and the coal seams removed by erosion. Coal occurs in the Serowe and Morupule Formations of the lower Ecca Group and is concentrated in four principle seams, namely the UMH, Z3, Z2 and Z1 seams. The sub-surface distribution of these seams has been investigated with the use of geophysical techniques, including aeromagnetics and wireline logging of exploration boreholes.

Magmatic activity dated ~180 Ma heralded the breakup of Gondwanaland and caused the Karoo basins to be intruded by dolerite sills, which had a profound effect on the coals therein. The first major effect was devolatilisation or burning of the coal as the dolerite intruded. The second major effect involved an increase in coal rank from sub-bituminous to bituminous or anthracite, as the temperature and perhaps pressure increased, due to the intrusion. Both these changes occurred on a relatively small scale, mainly affecting coal close to the intrusions. The third and last effect due to sill emplacement was metasomatism, which was caused by the elevated temperatures promoting fluid flows in the country rock on a much larger scale, as the fluids were able to migrate beyond the zone of conductive heat transfer. An important component of the metasomatic activity was the introduction of minerals such as calcite that precipitated in fractures and cleat systems in the coal, as the fluids moved through them. These minerals act as cement, thereby further reducing the permeability in an already tight reservoir.

Overall, the effects of the dolerite sills that have intruded in the area have been a negative one, affecting the coals adversely. The coals have become devolatilized, heat affected, or metasomatised, and their permeability reduced. These factors decrease the quality of the reservoir, and impact negatively on the possibility of a Coalbed Methane (CBM) project in zones containing igneous intrusions. It was noted that the distribution of dolerite intrusions at depth could only be partly determined from magnetics, because of the masking effect of the overlying volcanics, and it was necessary to make use of wireline logs and coal properties to assess the CBM potential.

Acknowledgements

I would like to take this brief moment to thank those who have helped me in both fulfilling my role as an MSc. student in petroleum geology, and completing this project.

The first group of people I would like to thank are my supervisors, Dr Russell Bailie at UWC and Professor David Reid at UCT. The two of you have been wonderful in your help, advice and prompting. Thank you for giving your time and help to a humble student.

Secondly, thank you to my parents and family. You have all brought me this far in life, and given me the opportunity to complete my student career with an MSc. degree (for now). Thank you for your love and support.

To the ladies and gentlemen at Sasol Petroleum International (SPI), especially Junior Potgieter, Alexie Milkov, Hanno van Staden and Jaques Roon. Without you gentlemen this project would be nowhere, and nothing. Thank you for your time, support and help – even when time was short.

From the bottom of my heart I thank you all.

Table of Contents

1. INTRODUCTION

Coalbed Methane or CBM, is a type of unconventional natural resource, and burns more cleanly than other fossil fuels (Halliburton, 2008). Southern African states use mainly coal for the generation of electricity (Zhou, 2012), although, the harsher environmental effects of burning coal has forced many countries to look to cleaner methods of providing energy. CBM takes advantage of the adsorptive property of coal, where methane is absorbed into the micropores or matrix within the coal, and, to a greater extent, is available as free gas within the macropores formed by cleats and other fractures (Aminian, 2005; White et al., 2005). Some methane is derived from biogenic processes in the low ranking (lignite and sub-bituminous) coals, with a larger portion of the methane being generated through thermal processes in the higher ranking bituminous coals (Halliburton, 2008; Al-Jubori et al., 2009) (Figure 1.1). Because the highest ranked anthracites are formed at high temperatures and pressures, the primary pore network, or cleats, is closed, and so, it is for this reason that the optimum coal rank for CBM is in fact sub-bituminous coal, and not the higher quality anthracite (Halliburton, 2008).

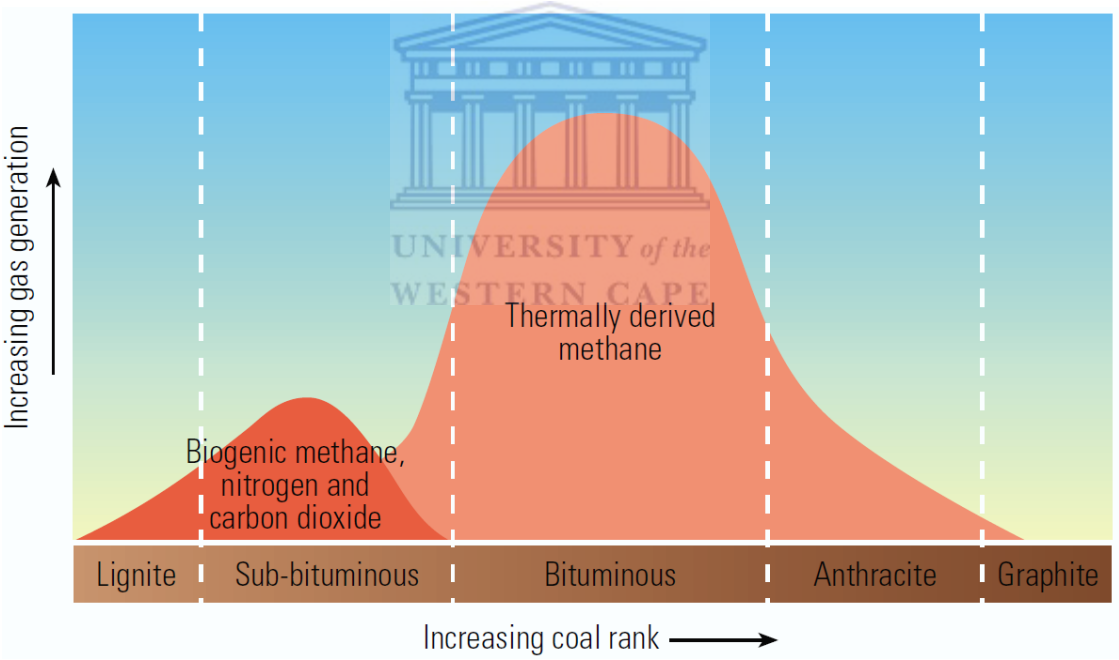

Figure 1.1: Methane is generated in coal by microbial bacteria through biogenic processes in lower ranked coals, or by heat through thermal processes in higher ranked coals. Biogenic methane may also form in higher ranked coals if fluid movement brings more microorganisms into the coal. From Al-Jubori et al. (2009)

1.1 Aims and Objectives

This study looks at the potential Coalbed Methane (CBM) reserves in three blocks located in Botswana, in the eastern portion of the Central Kalahari Sub-Basin (Figure 1.2.1). More specifically, it looks at the effect of the Jurasic dolerite intrusions on the Permian Ecca Group coals.

The major aims of this study are to:

1. determine the local geometry and distribution of the dolerite intrusion(s)
2. determine the effect of the dolerite on the coal

The overall objective is to determine and understand whether the coal is viable for the extraction of CBM, from the perspective of coal quality, and volatile matter, in order to aid exploration in the area. To achieve these aims, aeromagnetic, drill log and proximate analysis data from coal samples as well as core images will be used, in conjunction with a literature review.

1.2 Location

The study area consists of three blocks, Block A, Block B and Block C, from west to east, located about 75 km south-west of Francistown in Botswana (Figure 1.2.1). These three blocks are licensed out to Kubu Energy Resources and span an area of about 3000 km^2 (Potgieter, 2012) (Figure 1.2.1). The study area lies just south of the SW-NE trending Okavango Dyke Swarm, in the eastern portion of the Kalahari sub-basin, which forms part of the Larger Kalahari Karoo Basin.

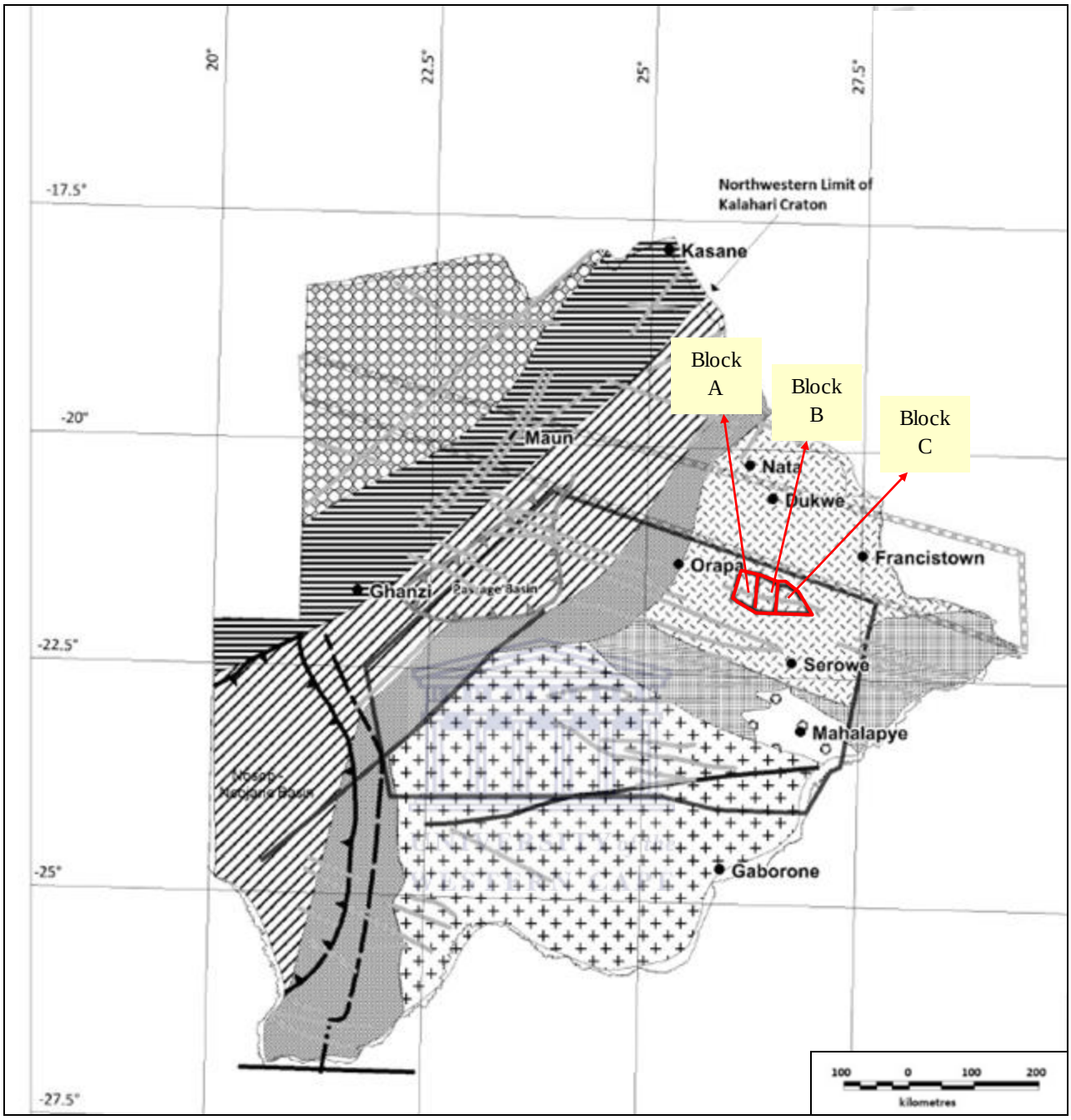

Figure 1.2.1: Location of the three Kubu Energy Resources blocks, Block A, Block B and Block C outlined in red, spanning an area of about 3000 km^2 (Adapted from: Potgieter and Anderson, 2012).

2. Literature Review

2.1 Basin Architecture

The Karoo basins of southern Africa formed and evolved due to the formation and breakup of Pangea (Catuneanu et al., 2005). The main Karoo Basin, in South Africa, is a retroarc foreland basin, which formed as a result of subduction to the south of Gondwana and associated flexural and dynamic loading (Catuneanu et al., 2005). At the same time, the Central Kalahari Sub-Basin formed as a result of thermal sagging, and was dominated by extensional or transtensional stresses (Catuneanu et al., 2005; Bennett, 1989). The Kalahari sub-basin is one of the Karoo sub-basins with a Karoo stratigraphy. Also, the Karoo basin is considered the type basin as it has the most complete succession within each group (Catuneanu et al., 2005). It is for this reason, as well as the proximity of the two basins that the deposited formations of both basins are comparable. However, understanding of the development of the Kalahari Karoo Basin is limited, and so theories on its formation is limited (Bordy et al., 2010; Catuneanu et al., 2005)

The Karoo Supergroup sedimentation ended with the break-up of Gondwana (Haddon and McCarthy, 2005) and the extrusion of the Drakensberg Lava Group. This was accompanied by the intrusion of dolerite dykes and sills (Haddon and McCarthy, 2005), with the Okavango dyke swarm occurring just north of the study area, at about 22°S (Bennett, 1989) and trending in a NW direction (Figure 2.1.1) (Potgieter and Anderson, 2012). Later, during the Late Cretaceous the Kalahari sub-basin experienced down-warping and uplift along epeirogenic axes, allowing the deposition of the Kalahari Group sediments (Haddon and McCarthy, 2005). The Kalahari Group sand covers about 70% of Botswana (Haddon, 2005) and most of the Karoo Supergroup (Bennett, 1989), with only a portion of the Karoo strata outcropping in the eastern portion of the country (Modie, 2007; Bennett, 1989; Smith, 1984).

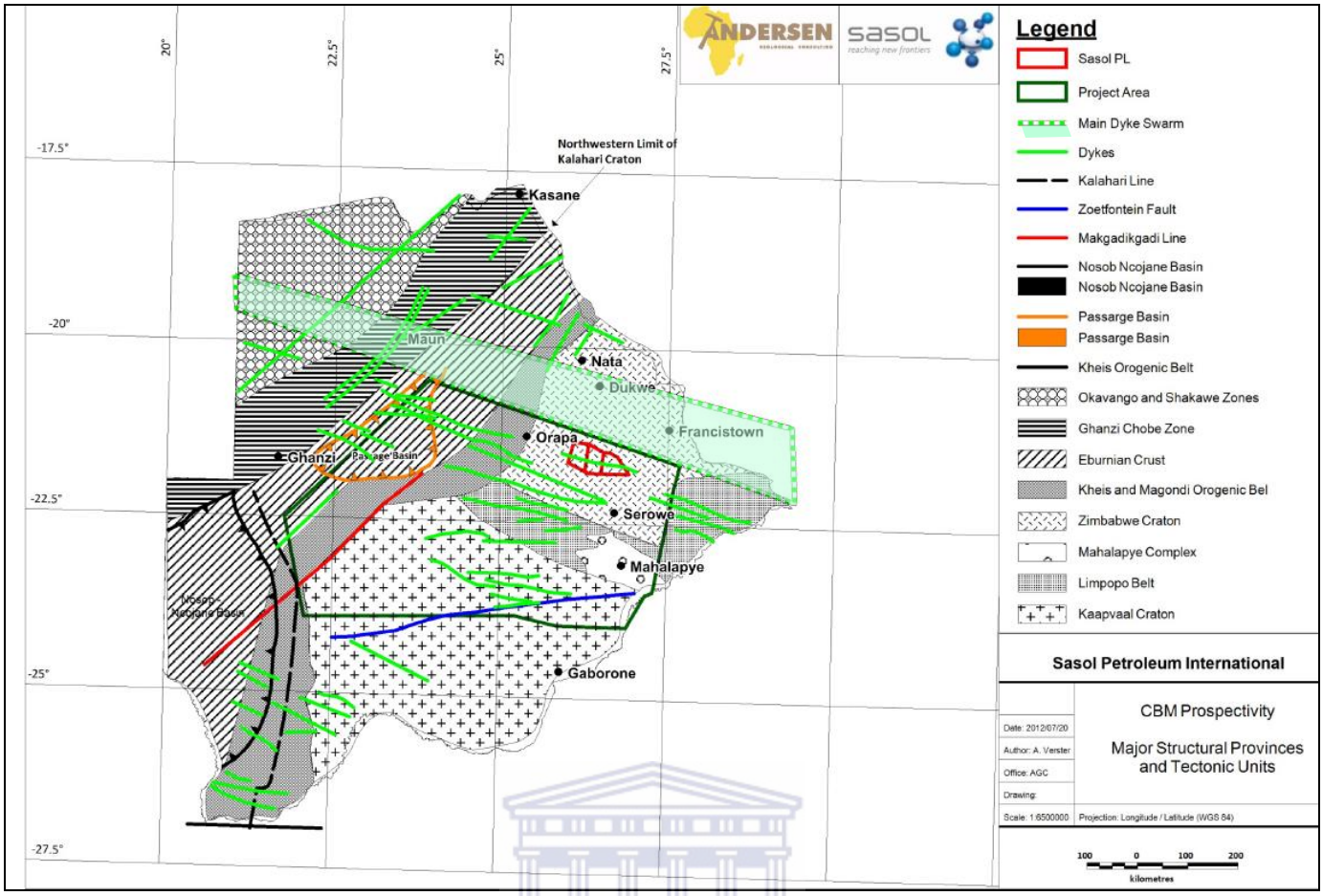

Figure 2.1.1: Location of the Okavango Dyke Swarm at 22°S, and trending NW-SE, with a general tapering-out to the west. (From Potgieter and Anderson, 2012)

2.2 Stratigraphy

Table 2.1.1 shows the various formations and groups found in the study area. Karoo deposition commenced with the Dwyka Group and its equivalent, the Dukwi Formation in Botswana, at about 300 Ma in the Late Carboniferous (Catuneanu et al., 2005), and is subdivided into a lower glacial tillite and an upper siltstone (Segwabe, 2008). In Botswana, the Dukwi Formation thins to the east, and is most well developed in the south-western portion of the country (Bordy et al., 2010; Smith, 1984).

The deposition of the Dukwi Formation was followed by the conformable deposition of the Permian Ecca Group sediments (Catuneanu et al., 2005), with the lower Ecca Group contact with the Dukwi Group being transitional (Visser, 1995). The Lower Ecca Group is a succession of dark coloured, siltstone beds deposited in a marine environment (Visser, 1995) with a maximum thickness of 107 m (Segwabe, 2008). The deposition of the Group began at about 288 ± 3 Ma (Bordy et al., 2010). The Middle Ecca Group consists of medium to coarse grained feldspathic sandstones, and coal seams (Smith, 1984). The coal seams occur predominantly in the eastern portion of the country, and tend to thin towards the west. The upper Ecca Group is defined by upward-coarsening fine-grained sandstone beds, deposited in a brackish deltaic environment (Visser, 1995).

Within the study area, the two main coal bearing units are the Serowe and Morupule Formations, with a maximum thickness of 50 m and 70 m, respectively (Bennett, 1989). These formations form the Middle to Upper Ecca Group (Smith, 1984)

The Tlhabala Formation was deposited above the Ecca Group during the Late Permian- Early Triassic (Catuneanu et al., 2005), and is bounded at the top and bottom by unconformities. This Formation has a maximum thickness of about 40 m (Segwabe, 2008). Scheffler et al. (2006) proposes that both the upper and lower unconformities were due to regional uplift, which led to some erosion of the previously deposited formation. The Tlhabala Formation consists of grey mudstone, siltstones, sandstones and thin limestone beds (Haddon, 2005). Catuneanu et al. (2005) propose that the Permo-Triassic Beaufort Group is restricted solely to the Main Karoo Basin of South Africa; however, the Tlhabala Formation of the Central Kalahari Sub-basin may be loosely correlated with the Beaufort Group across basins.

The Late Triassic-Early Jurassic Lebung Group forms part of the Upper Karoo Supergroup, and consists of red sandstones and mudstones (Bordy et al., 2010) as well as white to orange sandstones, which may be cross-bedded or massive (Segwabe, 2008). The uppermost sandstones are composed of rounded, frosted grains, indicating deposition under aeolian conditions (Segwabe, 2008). This Group has a maximum thickness of about 150 m, and is correlated with the Molteno, Eliott and Clarens Formations in the Main Karoo Basin in South Africa (Segwabe, 2008). The Lebung Group is composed of the lower Mosolotsane and upper Ntane Formations. In the eastern portion of Botswana, the Ntane Formation forms the local aquifer (Haddon, 2005). The less permeable Mosolotsane Formation is found between the aquifer, above it and the coal-bearing formations below it, causing it to act as an aquiclude.

The volcanic Stormberg Lava Group is equivalent to the Drakensberg Group in South Africa (Johnson et al., 1996), and lies above the Lebung Group (Segwabe, 2008), with an unconformity between the two Groups. The extrusion of this continental flood basalt occurred in the Late Jurassic due to the final breakup of Gondwana at about 180 Ma (Catuneanu et al., 2005; Bordy et al., 2010). The volcanics now have a maximum thickness of about 400 m in the Central Kalahari Sub-Basin (Segwabe, 2008).

The Kalahari Group Sands were deposited in the down-warped Kalahari Basin (Haddon and McCarthy, 2005). The Late Cretaceous to Quaternary sediments of this group were, and still are, being deposited by fluvial and aeolian processes, and as such are characterised by gravels, sands and silty sediment (Haddon and McCarthy, 2005).

Table 2.1.1: The stratigraphic table of the Waterberg, Central Kalahari (highlighted), and the Main Karoo Basins (From Potgieter, (*Pers Comm)* 2013 based on Smith, 1984)

Age	Group	Formation				
		Waterberg (Johnson *et al.* 1996)	Waterberg (Anglo Coal)	Central Kalahari (Smith, 1984)	Main Karoo Basin (Catuneanu *et al.* 2005)	Expected Thickness (m)
Jurassic	Drakensberg	Letaba		Stormberg Lava	Drakensberg	0 - 105
Triassic	Stormberg (South Africa) / Lebung (Botswana)	Clarens		Ntane	Clarens	55 - 120
		Lisbon	Elliot	Mosolotsane	Elliot	30 - 110
		Greenwich	Molteno		Molteno	
	Beaufort	Eendrachtpan	Beaufort Mudstones	Tlhabala	Driekoppen / Verkykerskop / Normandien / Volksrust	60 - 120
Permian	Ecca	Grootegeluk	B S 1 Seam	Serowe	Vryheid	5 - 20
		Swartrand	Ecca Seams	Morupule		35 - 85
		Wellington		Kamotaka	Pietermaritsburg	0 - 40
				Makoro		Not Intersected
Carboniferous	Dwyka	Wellington	Dwyka	Dukwi	Dwyka	5 - 37

2.3 Depositional Environment

The Dukwi Formation is a tillite and siltstone formation and, as such, it is interpreted to have been deposited in fluvioglacial and glaciolacustrine settings over present day Botswana (Scheffler et al., 2006; Visser, 1995). The Permian Dukwi sediments indicate a change in climatic conditions, from cold and dry to warmer climes (Visser, 1995). This can be correlated to the northward shift of Gondwana away from the South Pole. The Ecca Group Sequence is interpreted as being deposited within a shallow lacustrine environment, which graded into deltaic and even fluvial environments. Scheffler et al. (2006) explains that the large lacustrine environment was in-filled by Ecca Group sediment, such that the depositional environment evolved from a pro-delta with muds to one of more arenaceous sediments. The coal deposits formed during periods of subsidence in the basin, leading to the formation of swampy lacustrine systems (Smith, 1984) where plant life was allowed to flourish. The overlying Tlhabala Formation is interpreted to have been deposited in a lacustrine, environment (Visser, 1995; Smith, 1984), while the Late Triassic-Early Jurassic Lebung Group sediment was

deposited in fluvial conditions, forming the Mosolotsane Formation. These conditions eventually graded into an aeolian setting, which deposited the Ntane Formation (Bordy et al., 2010). The final group in the Karoo Supergroup, the Drakensberg Group, was extruded due to the breakup of the Gondwana Supercontinent.

The Kalahari Group is a superficial cover deposited by mainly braided fluvial systems, and as conditions changed to a more arid state, by aeolian systems. As such, the present day sediment is unconsolidated, and extensive (Haddon and McCarthy, 2005).

2.4 Tectonic Environment

Smith (1984) defined the boundaries of the Central Kalahari Karoo sub-basin as tectonic boundaries. These are the Zoetfontein Fault and Limpopo Mobile Belt, both of which lie south of the study area, the Okavango Dyke Swarm, to the north of the study area, and the Kalahari Line, to the west. The formation of these tectonic boundaries is due to the extension and wrenching of the basin, which occurs to the breakup up of Gondwana.

The 1500 km long, 100 km wide Okavango Dyke Swarm (Le Gall et al., 2002), or ODS, is located immediately north of the study area. The dykes are composed of dolerites and gabbros, dipping at 60° - 90° NE or SW (Le Gall et al., 2002). On a whole, the ODS trends at 110°E, and is wider in the east, and tapers off to the west (Figure 2.1.1). Le Gall et al. (2002) have interpreted this to mean a westward propagation of the dykes, away from the source region (Figure 2.4.1). Le Gall et al. (2002) also note that the dykes have striations akin to those of reverse faults, thus indicating that the dykes intruded through the fault, along the path of least resistance. The dyke swarm was emplaced within a 1 – 2 million year period (Le Gall et al., 2002) due to the breakup of the supercontinent Gondwana. Smith (1984) used the Okavango Dyke Swarm as the northern limit of this part of the basin.

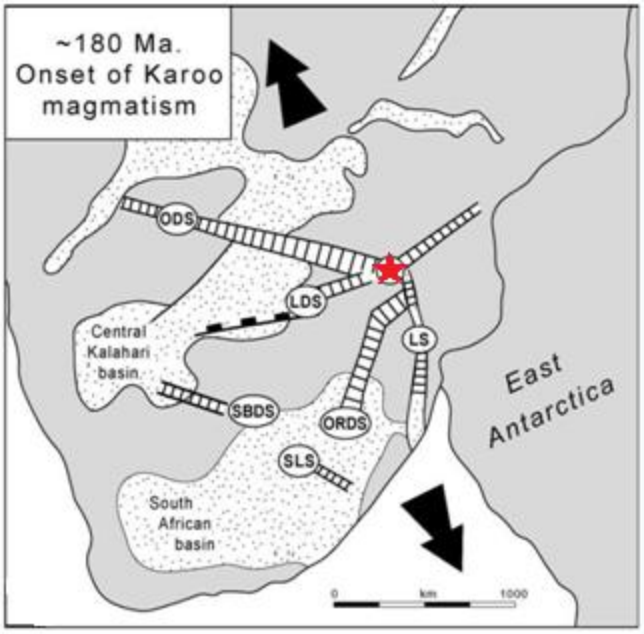

Figure 2.4.1: The Okavango Dyke Swarm (ODS) tapers off to the west and is interpreted as a westward propagation from the source, at Nuanetsi represented by the star. ODS: Okavango Dyke Swarm; LS: Lebombo Dyke Swarm; ORDS: Olifants River Dyke Swarm; SBDS: South Botswana Dyke Swarm; SLS: South Lesotho Dyke Swarm. The arrows represent direction of extension during rifting From: Le Gall et al., 2005)

The Limpopo Belt lies south of the study area (Figure 2.1.1), and was formed due to the collision of the Kaapvaal and Zimbabwe cratons during Proterozoic times (James et al., 2003). The Limpopo Mobile Belt trends in a northwest-southeasterly direction and is composed of mainly gneisses and granites from the adjacent cratons.

The east-northeast – west-southwest striking Zoetfontein Fault marks the southern boundary of the Central Kalahari basin (Figure 2.1.2) (Smith, 1984). The Zoetfontein Fault formed during the formation of the Kheis and Magondi Mobile Belts between 2100 and 1800 Ma (Smith, 1984) but further south of the Limpopo Belt. The Zoetfontein Fault was reactivated during Karoo sedimentation, and developed as a growth fault (Modie, 2007).

The Passarge and Nosob Ncojane basins are located west and south-west of the study area respectively (Figure 2.1.1). These basins formed during Karoo times as a result of enhanced sagging in these localities (Bennett, 1989), but according to the ARI (2003) the coal here is found to be at a depth of 1000 m or greater – too deep for CBM, as the coal would be metamorphosed and highly pressurised, if not metasomatised.

2.5 Coal

Coal is a "solid, brittle, combustible, carbonaceous rock formed by the decomposition and alteration of vegetation by compaction, temperature and pressure" (Speight, 2005). Coal is formed by woody and moss plant material, which is deposited in swampy areas, with a low oxygen content (Boggs, 2010). The peat that forms is eventually compacted and metamorphosed by pressure and heat into a coal (Speight, 2005) by the process of coalification (Halliburton, 2008). The most important element of this process is heat, which allows the organic matter to break down, forming coal and large volumes of gas, which are then adsorbed by the macro and micropores (Halliburton, 2008). Varying degrees of metamorphism and compaction lead to different ranks of coal, with, from lowest to highest, with increasing metamorphism, these being lignite, sub-bituminous coal, bituminous coal and anthracite (White et al., 2005; Speight, 2005). A burial depth that corresponds to a temperature of 212-300 °F (100 – 149 °C) leads to the formation of bituminous coal (Halliburton, 2008), with lower temperatures causing the coal to remain as sub-bituminous coal and even lignite. With a greater degree of compaction there is a greater loss of volatile matter from the coal (Speight, 2005), and the best coal for CBM is a bituminous coal rank as this is the highest grade of coal with a good cleat system and ability to fracture (Halliburton, 2008). Higher ranks, such as anthracite, have a lower permeability due to the higher pressures to which the coal has been subjected.

Heat, one of the major factors that affect the coalification process (Halliburton, 2008), may be brought about by burial, radioactivity and/or volcanic activity (Halliburton, 2008). Burial affects the temperature of the coal on a basin-wide scale, whereas igneous intrusions and radioactive material may only have a local effect on the coal, (Halliburton, 2008). This study did not look at the effect of radioactive elements on the coal, due to time and data constraints. The dolerite sills that have intruded in the area, however, have played a role in the coalification process due to the magmatic heat involved.

Proximate analysis of coal determines the ash, volatile matter, moisture and fixed carbon content in weight percentages (wt. %) (Speight, 2005). This data can be used to establish the rank of the coal (lignite to anthracite) and the volatilization degree (Sasol, 2011). The volatile matter and moisture contents are not defining elements in coal rankings, as each coal rank displays a similar range in moisture and volatile matter by weight percent. Table 2.5.1 (after Speight, 2005) gives the ash, moisture, fixed carbon and volatile matter contents expected for the various coal ranks. Bituminous coals and anthracite can be further subdivided into groups based on the same property ranges given by the proximate analysis. These are given in Table 2.5.2.

Table 2.5.1: Expected composition and Property Ranges for Various Ranks of Coal (From: Speight, 2005).

	Anthracite	Bituminous	Subbituminous	Lignite
Moisture (%)	3–6	2–15	10–25	25–45
Volatile matter (%)	2–12	15–45	28–45	24–32
Fixed carbon (%)	75–85	50–70	30–57	25–30
Ash (%)	4–15	4–15	3–10	3–15
Sulfur (%)	0.5–2.5	0.5–6	0.3–1.5	0.3–2.5
Hydrogen (%)	1.5–3.5	4.5–6	5.5–6.5	6–7.5
Carbon (%)	75–85	65–80	55–70	35–45
Nitrogen (%)	0.5–1	0.5–2.5	0.8–1.5	0.6–1.0
Oxygen (%)	5.5–9	4.5–10	15–30	38–48
Btu/lb	12,000–13,500	12,000–14,500	7500–10,000	6000–7500
Density (g/mL)	1.35–1.70	1.28–1.35	1.35–1.40	1.40–1.45

Table 2.5.2: Subdivision of coal rankings (From: Halliburton, 2007).

		Fixed Carbon Limits (%, Dry, Mineral-Matter-Free Basis)		Volatile Matter Limits (%, Dry, Mineral-Matter-Free Basis)	
Class	Group	Equal to or Greater Than	Less Than	Greater Than	Equal to or Less Than
I. Anthracitic	1. Metaanthracite	98	—	—	2
	2. Anthracite	92	98	2	8
	3. Semianthracite[c]	86	92	8	14
II. Bituminous	1. Low-volatile bituminous coal	78	86	14	22
	2. Medium-volatile bituminous coal	69	78	22	31
	3. High-volatile A bituminous coal	—	69	31	—
	4. High-volatile B bituminous coal	—	—	—	—
	5. High-volatile C bituminous coal	—	—	—	—

The coals of the Ecca Group in Botswana are comparable to those in the Main Karoo Basin in South Africa (Bennett, 1989). The bituminous coals are generally inertinite, and have a high ash content. The coals have a high inherent moisture content and a medium calorific value (Bennett, 1989). Proxy data from the nine cores from the study area give average values for ash (29.96%), moisture (3.22%), volatile matter (24.36%) and fixed carbon (42.46%). The average vitrinite reflectance values (from the Mmamabula central area) indicate that the coals have undergone limited burial and subsidence (Bennett, 1989). A CBM study based on a limited number of cores in Botswana estimated that there is about 5.6 Trillion cubic meters (Tcm) of CBM reserves in the Central Kalahari Sub-Basin with a recoverable amount of 1.7 Tcm (Global Methane Initiative, 2011).

2.6 Effects of Dolerite Intrusions on Coal

The intrusion of dolerite magma causes contact metamorphism to the surrounding country rock due to the increased temperatures. This increase in temperature heats up the coal, and causes it to thermally decompose, or become devolatilised. Coalfields have been shown to have a lack of correlation between the size of the dolerite intrusion and the level of devolatilization of the coal (Golab and Carr, 2004), because the many emplacement factors of the dolerite regulate the metamorphic effect (Bussio, 2012). The emplacement factors for the dolerites are given by Bussio (2012) as the distance travelled by, and thus the temperature of the dolerite magma, the density of the magma, the flow rate of the magma, the magma chamber overpressures, the depth of emplacement and the flow regime within the conduit.

A second effect of a dolerite intrusion on coal is hydrothermal metasomatism due to fluids from the surrounding rock being heated. The heated fluids (about 100-200 °C) are very mobile and move through fractures in the coal, thereby causing devolatilization (Bussio, 2012) by dissolving out the volatiles of the coal. It is because of this high mobility that there is no linear relationship between the density of intrusions and the amount of devolatilization experienced by the coal.

When a coal becomes devolatilised, the ash content increases, while on the other hand, the volatile matter content decreases. Also, according to Golab and Carr (2004), thermally altered coal shows a variation in certain elements with the concentration of sodium (Na), aluminium (Al), and zirconium (Zr), amongst others, all increasing closer to the contact. Conversely, the concentration of elements such as silicon (Si), lanthanum (La) and neodymium (Nd), as well as others, decreases closer to the contact. This change in element concentration either towards or away from the contact is due to element mobility (Golab and Carr, 2004). Using these parameters, the extent of the devolatilised areas can be assessed and mapped. Golab and Carr (2004) also make one last valuable note, indicating that the mere presence of ankerite and siderite minerals indicate that the coal has been thermally altered,

and so these two minerals are a good petrographic way of identifying heat affected coal from unaltered coal.

3. Methodology

3.1 Aeromagnetic Data

The aeromagnetic data was supplied by Fugro (Kovac and Cevallos, 2012), and it is their interpretation used in this thesis (Figure A1 in Appendix A).

The aeromagnetic data shows a basalt cover over much of the study area, as well as mafic dyke intrusions through the basalt (Figure 4.1.1). The dykes follow the same NW-SE trend as the Okavango Dyke Swarm found along the northern border of the study area. Upper and lower sills were interpreted in the north-eastern part of the study area, and are thought to have been fed by the dykes in the area, although the exact relationship is yet to be found.

3.2 Core Images

Nine (9) cores were drilled over the entire study area, and the cores taken into the lab to be analysed and photographed. Unfortunately, the cores are in the keeping of the Botswana Government, where they were not available to access for this project. However, the core images taken in the field and in the lab were made available. The core images were helpful in correlating the wireline logs to the log reports for each of the boreholes, by matching up coals and dolerites at the appropriate intervals, as well as in correlating the formations found in each of the boreholes. It was also used to determine the location of quenched or chill margins of the dolerite intrusions.

3.3 Log Data

Log data was provided by Kubu Energy Ltd. in the form of a single spreadsheet for each borehole. This described each of the entire unslabbed cores, with special attention on the coal beds. It also included the top and bottom depths of each lithology, the formation to which the lithology belongs, and additional comments. The log data was incorporated with the IP generated logs in order to create the cross sections.

3.4 Wireline Data

The wireline log data were provided in .las format, and were displayed in the Interactive Petrophysics (IP) software package. Initially, the gamma-ray (GR) log coupled with the density log was used to define the stratigraphic position of each of the dolerite intrusions in each borehole. A dolerite intrusion was defined by a gamma-ray response of less than 60 API, and a density response of 2.67 g/cm^3 or more (Figure 3.4.1). The stratigraphic locations of the dolerites, as well as the formations

found within each borehole, as determined from log data, were displayed on IP. However, since this software is mainly a sedimentary based software package, the cross cutting relationships between the mafic intrusions and the sedimentary rock layers could not be displayed on IP. Therefore, each of the nine logs had to be exported as images displaying each formation, coal seam (also extracted from log data) and stratigraphic positioning of the dolerite intrusions. These were then used to create cross sections by hand, displaying the interpreted layered stratigraphy and crosscutting sills as a number of 2D images (AppendicesB1 and B2). A 2D representation was used in this case, as the images had to be created by hand, as there was no software available to create these.

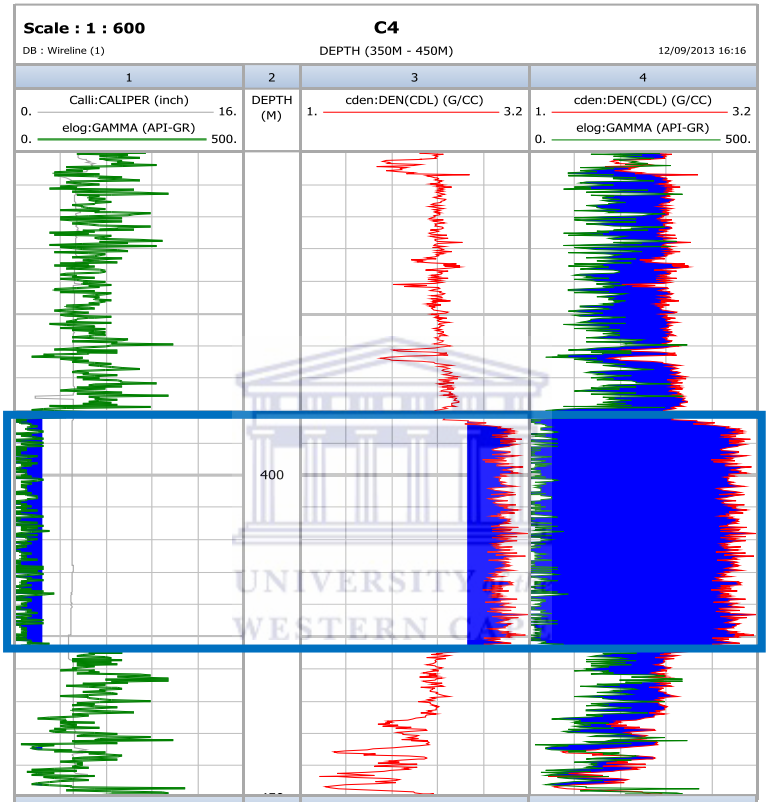

Figure 3.4.1: A section of the C4 borehole displayed on IP, displaying the stratigraphic location of a dolerite intrusion, identified by a combination of a GR reading of less than 60 API, and a density of more than 2.67 g/cm^3. The dolerite intrusion is identified in this figure by the blue box.

3.5 Proximate Analysis Data

The proximate analysis on each of the coal samples, for each borehole, was done by Weatherford Laboratories, while sapling was done by Sasol. Weatherford then supplied the air dried ash, moisture, volatile and fixed carbon contents of the coal. In some cases the coal was interbedded with mudstone, and/or carbonaceous mudstone. This sullied the data for those particular samples, which were then interpreted and categorised as "non-coal". The data from the pure coal samples were preferentially used to determine the rank of the coal, or whether the coal had been devolatilised, according to the following categories:

ELEMENT	RANGE	INDICATES
Ash Content	>36 wt. %	Devolatilised Coal
Ash Content	3 – 10 wt. %	Bituminous Coal
Fixed Carbon Content	50 – 70 wt. %	
Ash Content	4 – 15 wt. %	Anthracite
Fixed Carbon Content	75 – 85 wt. %	
Ash Content	➢ >36 wt. % ➢ Abundant calcite &/ or highly fractured ➢ No Dolerite occurring stratigraphically close	Metasomatised Coal
Volatile Content	< 16 wt. %	Devolatilised Coal

4. Results

4.1 Aeromagnetic Data

Aeromagnetic data covering the study area (Figure 4.1.1) were gathered and interpreted by Fugro Airborne Surveys (Kovac and Cevallos, 2012) (Figure 4.1.1). Since the Karoo sedimentary rocks do not show a magnetic signature, the lithologic interpretation of the magnetic data emphasizes the distribution of the overlying basaltic igneous rocks. The basalt covers the sedimentary rock of the Karoo Supergroup strata, while intrusive sills can be detected along the northern boundary, and in the eastern portion of the study area, but only due to the absence of the basalt cover, so intrusions may extend further, under the basalt cover. A younger dolerite dyke system is also evident in the magnetic data where it intrudes through the basalt cover, usually along the WNW trending fault system (Haddon and McCarthy, 2005).

Using the fault system within the study area, the 3 license blocks can be sub-divided into six (6) tectonic blocks, named here (from south to north) as Blocks 1 – 6 (Figure 4.1.2). These faults formed during the collision of the Kaapvaal and Zimbabwe cratons, and have been re-activated during the emplacement of the Okavango Dyke Swarm (Kovac and Cevallos, 2012).

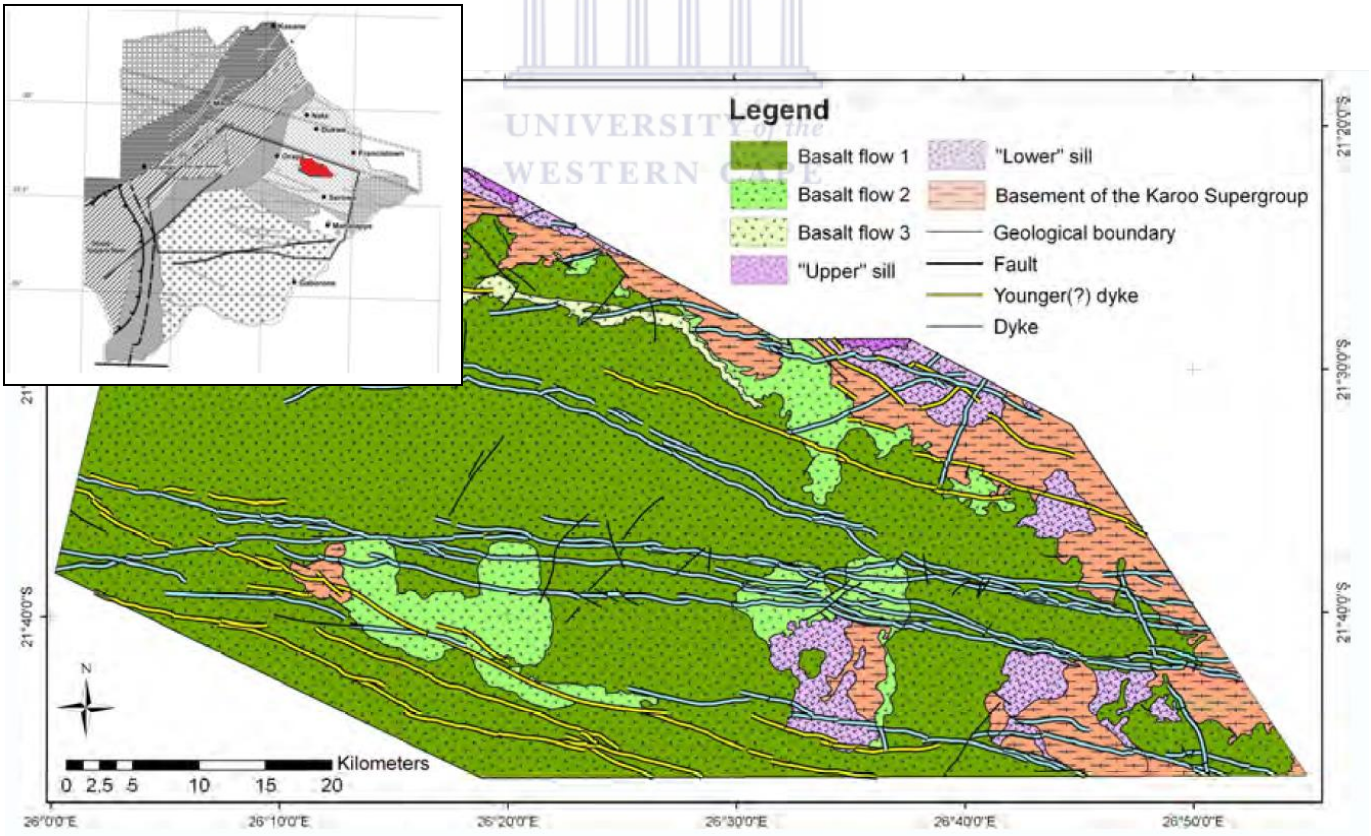

Figure 4.1.1: Lithological interpretation of aeromagnetic data covering the study area. The masking effect of the basalts (green) hampers the ability to detect the underlying dolerite, and only the dolerite dykes cutting the lavas can be shown. However, an upper and a lower dolerite sill (in purples) are evident in the areas where the basalt cover has been eroded. Inset is the location of the three exploration blocks in red. (See also Figure A1). From Kovac and Cevallos (2012).

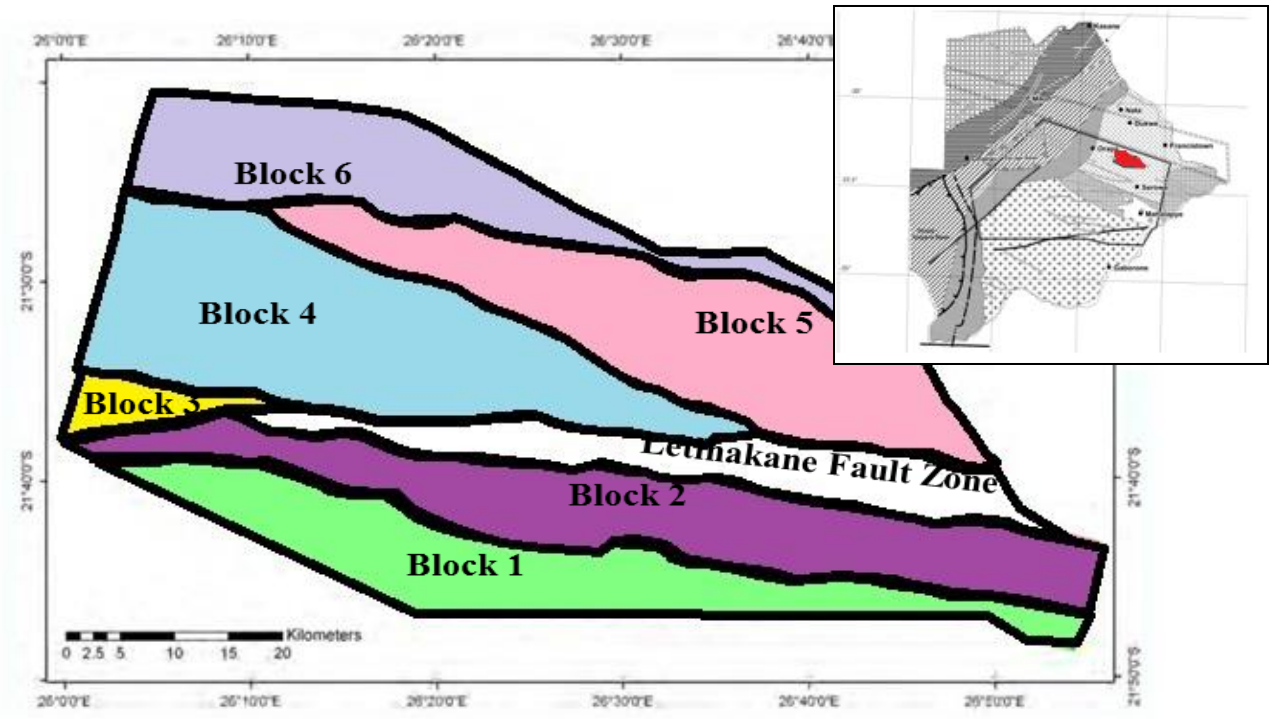

Figure 4.1.2: Subdivision of the study area into six blocks (Blocks 1 – 6) defined by the WNW fault system seen in Figure 4.1.1.

4.2 Wireline Data

North-south and west-east cross sections (Appendices B1 and B2) were constructed taking into account the stratigraphy inferred from the downhole log and wireline data (Figure 4.2.1) as discussed in section 3.4.

The cross sections show that the sills are confined to the Morupule and Serowe Formations, and cut obliquely across the coal seams. This shows that the sills intruded along the path of least resistance causing the coal seams in its path to be either displaced or consumed.

In some cases, as in borehole C2 (Figure 4.2.2), the dolerite displaces the coal and causes thickening of the host formation, in this case the Morupule Formation, which is 50 m thicker than expected, due to the presence of the 50.45 m thick dolerite sill. Figure 4.2.3 (and figures in Appendix B2) shows that the dolerites either cut across or moved parallel to the coal seams. This lateral continuity of the sills, especially those close to the coal beds is assumed to have caused wide spread thermal alteration to the coal.

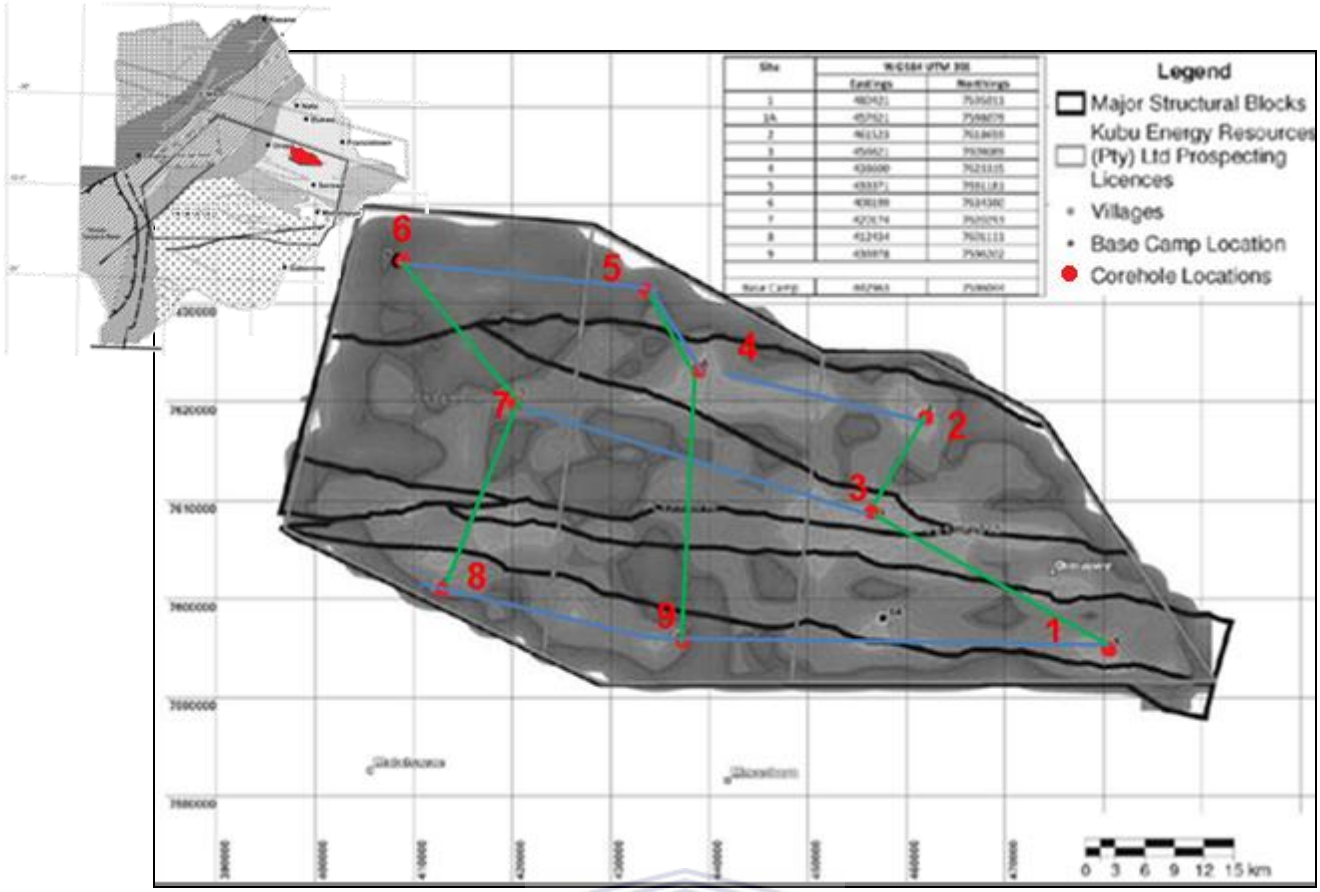

Figure 4.2.1: Location of the 9 boreholes used in this study, with blue lines representing west-east cross sections and green lines representing north-south cross sections created. The inset shows the location of the three exploration blocks. (Adapted from: Potgieter, 2012).

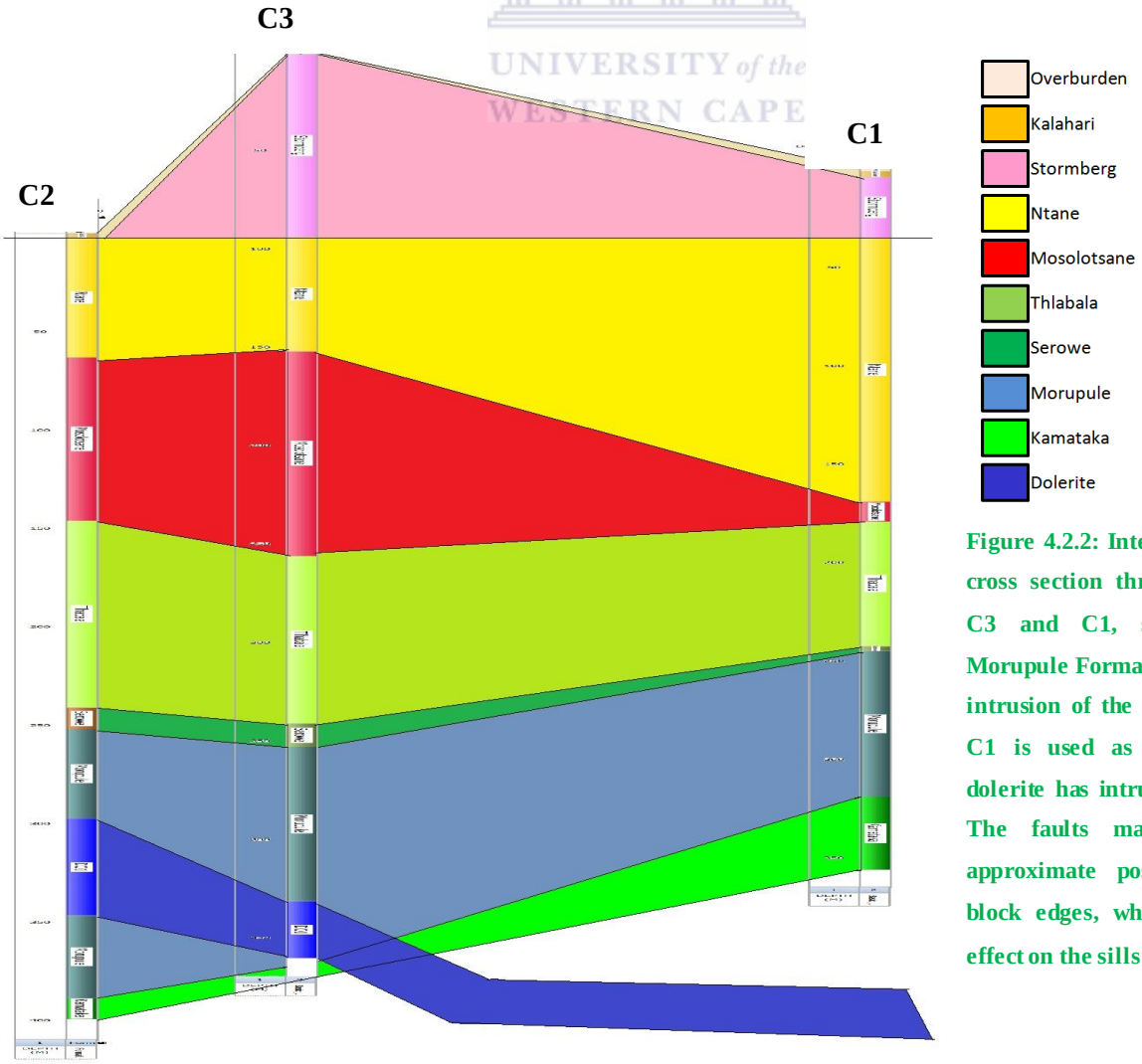

Figure 4.2.2: Interpreted north-south cross section through boreholes C2, C3 and C1, shows the thicker Morupule Formation in C2 due to the intrusion of the dolerite (dark blue). C1 is used as the control as no dolerite has intruded in this vicinity. The faults marked indicate the approximate position of the fault block edges, which have no major effect on the sills

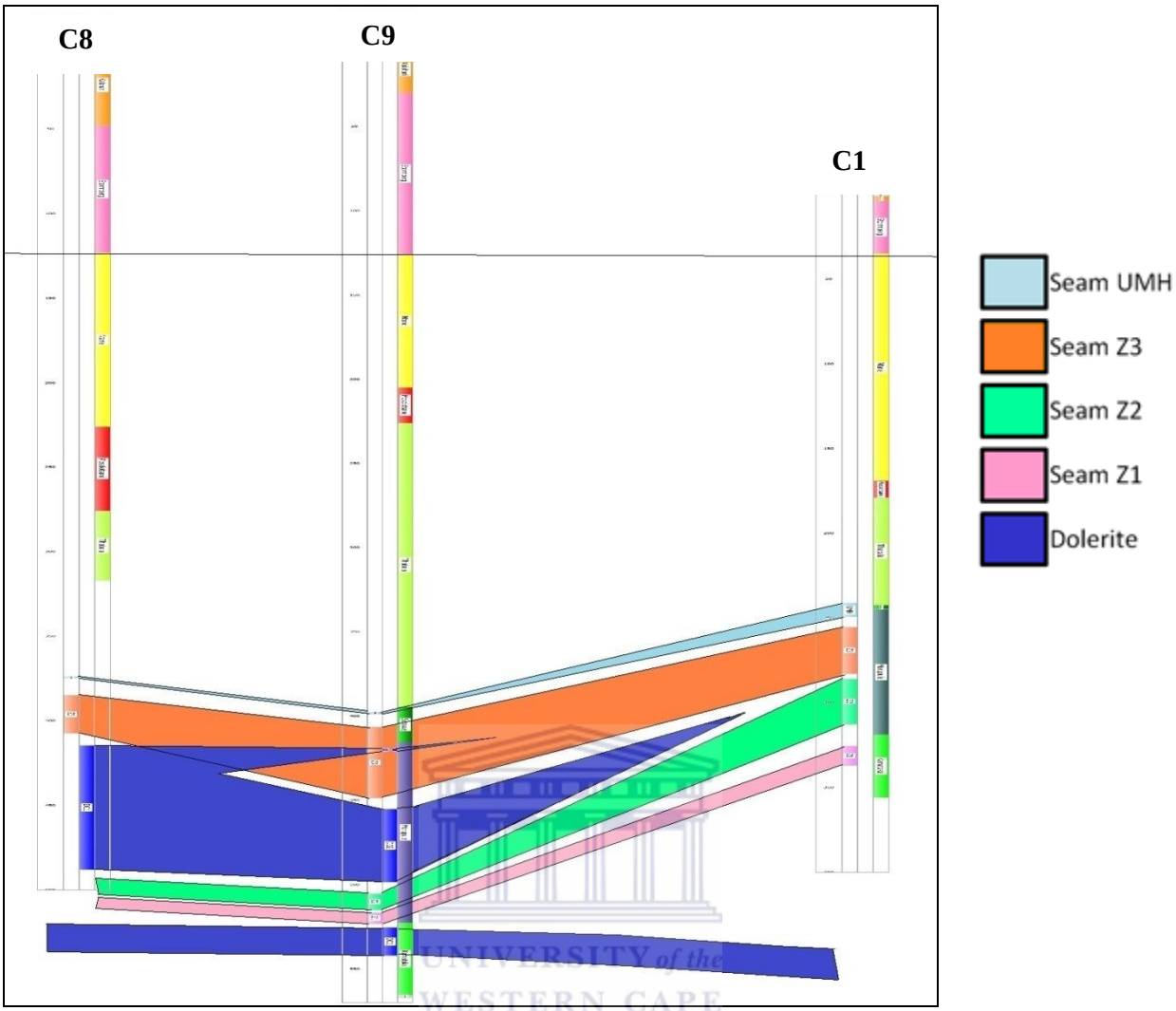

Figure 4.2.3: West-east cross section created from boreholes C8, C9 and C1, with the base of the Stormberg Group used as the datum. The dolerite sills cut through seamZ3, from the Morupule Formation between C9 and C8, and in between seams Z3 and Z2, both from the Morupule Formation, between boreholes C9 and C1.

4.3 Proximate Analysis Data

Proximate analysis data were provided for each ply, or coal sequence by Weatherford, from the Serowe and Morupule Formations (Table 4.3.1 and Appendix B3). The ash, moisture, volatile matter and fixed carbon content were provided for each sample, along with a detailed log description, and were used to determine the coal rank. The degree of devolatisation was determined by the criteria given in section 3.5, while the coal rank was determined by the following criteria:

ELEMENT	RANGE	COAL RANK
Fixed Carbon Content	>50 wt. %	Bituminous Coal
Moisture Content	< 25 wt. %	
Fixed Carbon Content	30 – 50 wt. %	Sub-bituminous Coal
Fixed Carbon Content	>70 wt. %	Anthracite
Log description of "bright coal" and "visible vitrinite"		

In some cases mudstone and carbonaceous mudstones were included in the coal sample used in the analysis. These were recorded from the log and defined as "non-coal" sediment. However, the logs were still used in order to determine if this sediment was affected by intruding dolerite, where comments such as "baked" and "devolatilised" indicate that the sediment, be it mudstone or coal, has been heat affected.

Table 4..3.1: Proximate analyses of coal samples from the Z1, Z2, Z3 and UMH coal seams of the Morupule and Serowe formations from borehole C2, with the stratigraphic position of the dolerite intrusion displayed, as well as the coal rank for each sample.

Sample Number	Formation	Top Depth	Bottom Depth	Moisture	Ash	Volatile Matter	Fixed Carbon	Seam	Rank
		(m)	(m)	(%)	(%)	(%)	(%)		
D01	Serowe	251.25	251.81	3.07	91.07	5.69	0.17	Z3	Non-coal
D02	Serowe	252.12	252.72	4.81	34.96	29.07	31.17	Z3	Subbit
D03	Serowe	257.64	258.25	4.88	26.79	33.52	34.82	Z3	Subbit
D04	Serowe	262.62	262.94	5.28	18.96	32.10	43.66	Z3	Subbit
D05	Serowe	263.97	264.30	5.13	25.06	29.76	40.05	Z3	Subbit
D06	Serowe	266.26	266.68	5.14	20.48	30.30	44.08	Z3	Subbit
D07	Serowe	272.49	273.09	2.69	26.84	27.69	42.78	Z3	Subbit
D08	Serowe	273.09	273.36	2.32	22.51	28.21	46.96	Z3	Subbit
D09	Serowe	276.51	276.74	1.45	21.45	16.30	60.81	Z3	Bit
D10	Serowe	278.16	278.49	1.00	34.77	17.08	47.15	Z3	Bit
Dolerite at: 295.26 - 354.71 m									
D11	Serowe	357.97	358.27	0.76	34.45	18.77	46.02	Z2	Bit
D12	Serowe	378.71	379.01	5.06	23.67	25.11	46.16	Z2	Subbit

4.4 CORE PHOTOS

Images of the unslabbed cores from all nine boreholes were taken, and provided by Kubu Energy, while the cores were still in the field (Figure 4.4.1 and Appendix A2). These had the coal intersections already removed from the trays, so were not informative in determining the rank of each coal bed. However, the dolerite and sedimentary rocks in contact with the intrusion were recorded, and these were used in conjunction with the log data to determine whether the dolerite had caused any heat

damage. Photos of the coal samples in boreholes C3, C6 and C7 (Figure 4.4.2 and Appendix A3) that were used in the proximate analysis were made available for this study.

Bright coal usually indicates a higher coal rank, where the vitrinite may actually be seen with the naked eye, such as in anthracite, whereas dull coal is indicative of a lower rank, including not only bituminous and sub-bituminous types, but also devolatilised coals. The distinction between the three may be made using the proximate analysis as well as log data.

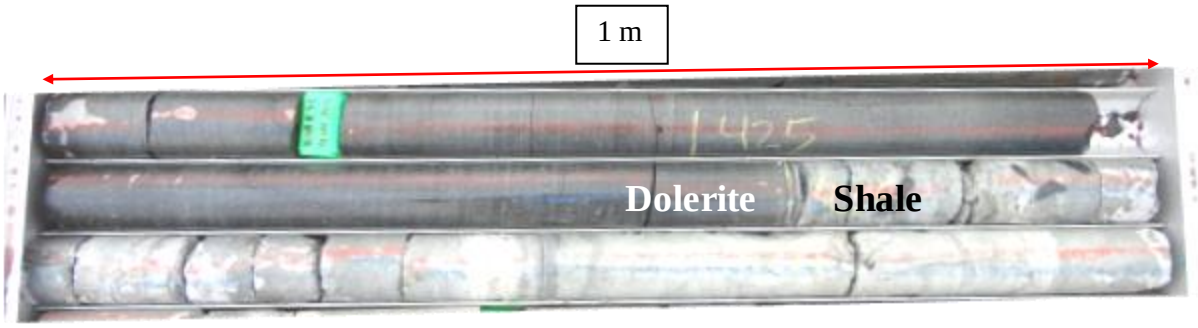

Figure 4.4.1: Core photo from borehole C4, showing the bottom contact of the dolerite (dark) against shale (light) at a depth of 426 m. The hardness and brittleness of the shale, as well as the discolouration is attributed to the effect of the heat from the dolerite intrusion. (Image provided by Kubu Energy).

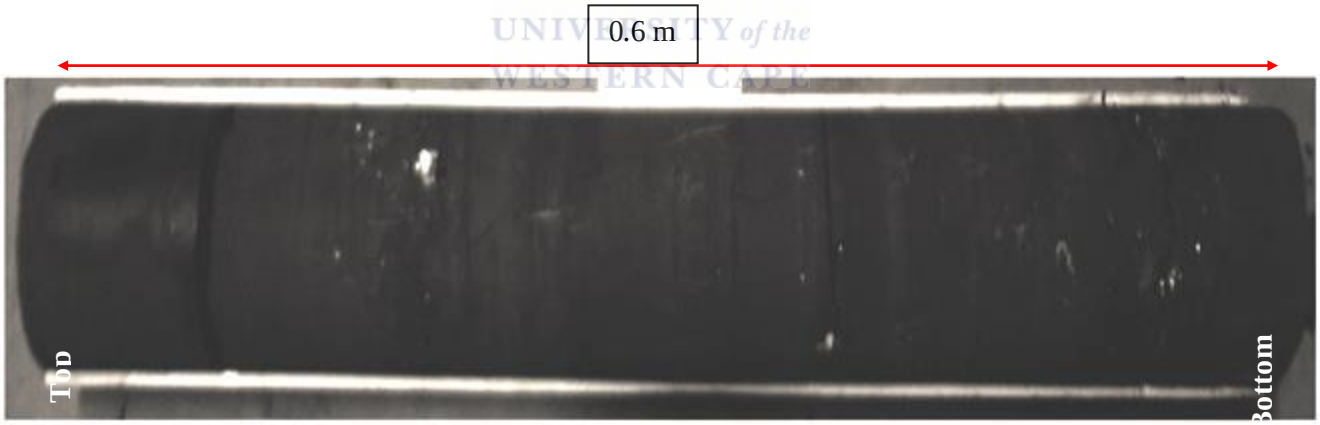

Figure 4.4.2: Dull devolatilised coal sample taken from a depth of 485.62 m to 486.22 m from borehole C7 (Image provided by Kubu Energy).

5. Discussion

5.1 Aeromagnetic Data

Much of the 3000 km^2 study area is covered by Stormberg Lava Group, which magnetically veils the underlying lithologies and structure (Kovac and Cevallos, 2012) by its mottled, or spotted, texture. Various mottled textures indicate the different flows, labeled here as Basalt Flow 1 -3, and indicated in Figure 5.1.1 in green hues. Only in a few localities has the basalt cover been removed by erosion, allowing the magnetic signature of subsurface dolerite sills to be detected with confidence (Figure 5.1.1). One of these two areas, or windows, is located in the south west portion of the study area, and the second of these two is located in the southeast portion of the study area. These erosional windows are not large, but the presence of these intrusive sills is confirmed through the aeromagnetic data by Kovac and Cevallos (2012), and it is therefore probable that they are continuous throughout the study area.

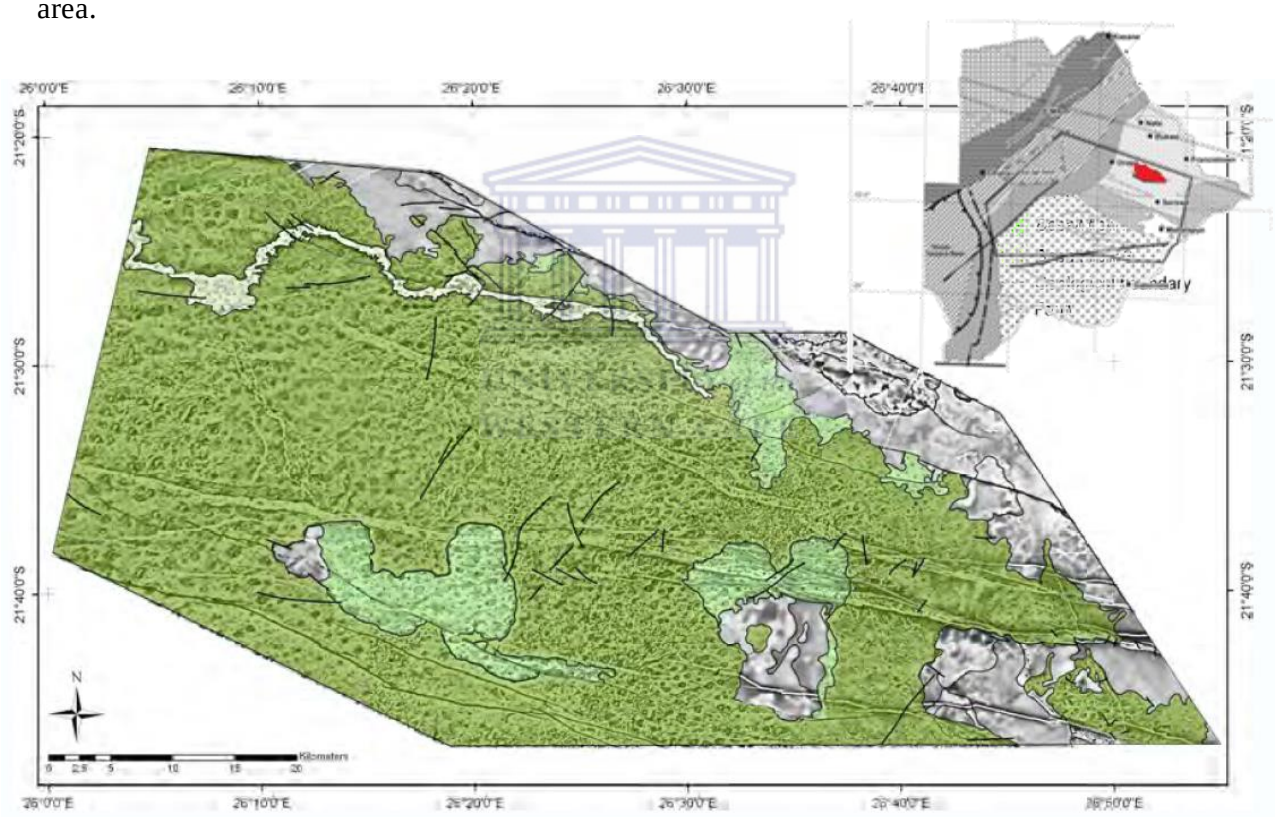

Figure 5.1.1: The mottled texture of the overlying basalt (shown in green shades) obliterates the magnetic response of the underlying geology, making identifying the dolerite sills and dykes impossible where there is a basalt cover. From Kovac and Cevallos (2012).

Linear anomalies cutting across the mottled pattern caused by the basalts (Figure 5.1.1) have been interpreted as the magnetic response caused by dolerite dykes and faults that crosscut the basalts (Figure 5.1.2 and Appendix A1).Some of the dykes show en echelon patterns (inset of Figure 5.1.2), following the fault through which they intruded. The fracture system was caused due to wrenching during the break-up of Gondwana (Catuneanu et al., 2005; Potgieter and Anderson, 2012). This en-

echelon pattern indicates that some of the dykes post-date the Stormberg Lava Group, at 178.4 ±1.1 Ma (Jourdan et al., 2004).

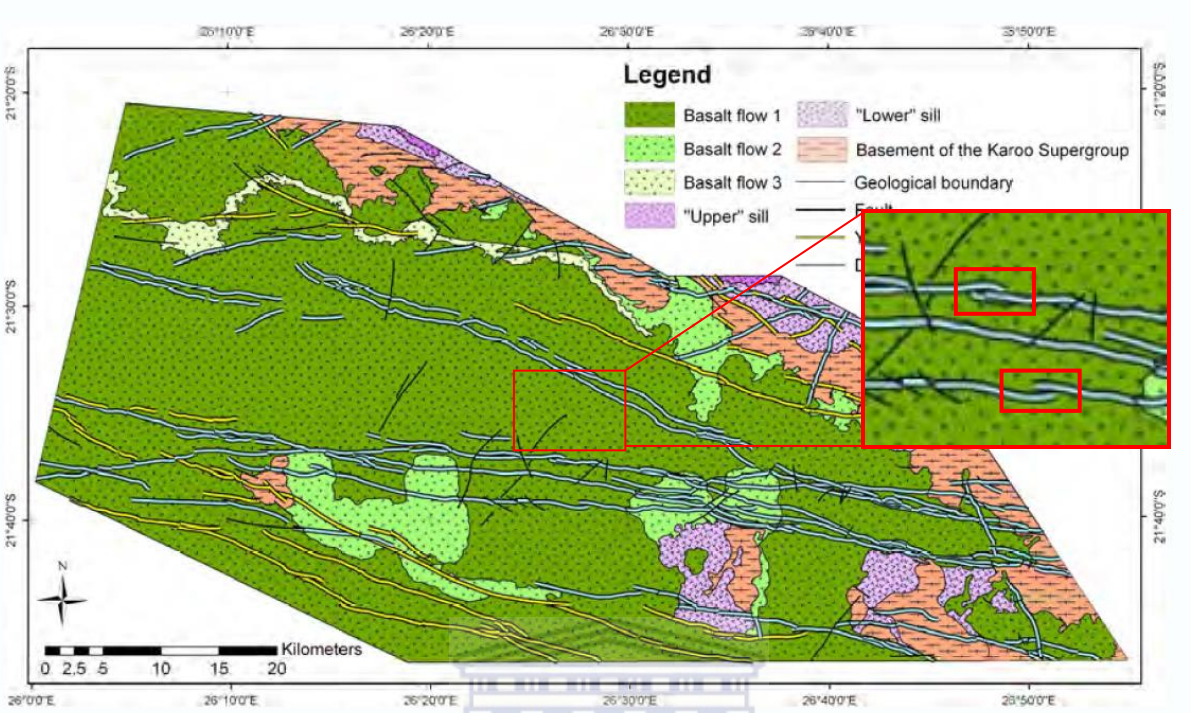

Figure 5.1.2: Geological interpretation of the magnetic survey shows dolerite dykes (blue lines) intruding through the overlying basalts (greens). The dykes took a path of least resistance through the pre-existing faults in some cases. The inset image is a blowup of the boxed area showing the dykes taking on an en echelon shape, as it intruded through faults. Adapted from Kovac and Cevallos (2012).

The aeromagnetic data has also been interpreted to show two mafic sills in the northeastern part of the study area, termed here the "Upper Sill" and the "Lower Sill" (shown in two shades of purple in Figure 5.1.2). Windows eroded through the basalt covering the southern part of the study area show only the Upper Sill, although this could be due to another veiling effect affecting the underlying lithologies and structures. This is also shown in the following cross sections (e.g. Figure 5.2.1).

5.2 Cross-Sections

A number of cross-sections were created (Appendix B1) in order to understand the geology of the study area, with particular emphasis on the cross-cutting relationships of the intruding dolerite sill(s) and the Karoo Supergroup. The cores were plotted with relative distances taken into account, with the top of the Ntane Formation used as the datum surface (Figure 5.2.1). This is because the base of the basalts is a pre-eruption surface. A second cross section (Figure B1.8) was also created, using the top of the Tlhabala Formation as the datum. From the cross sections, or borehole correlations, created using all nine boreholes (Figure 5.2.1 and Appendix B1), each formation was interpolated between the

wells, and the geometry of the dolerite sills were deduced. Other cross sections were again created, following the same trajectories, with these displaying the four coal seams and dolerite sills (Figure 5.2.2, Appendix B2).

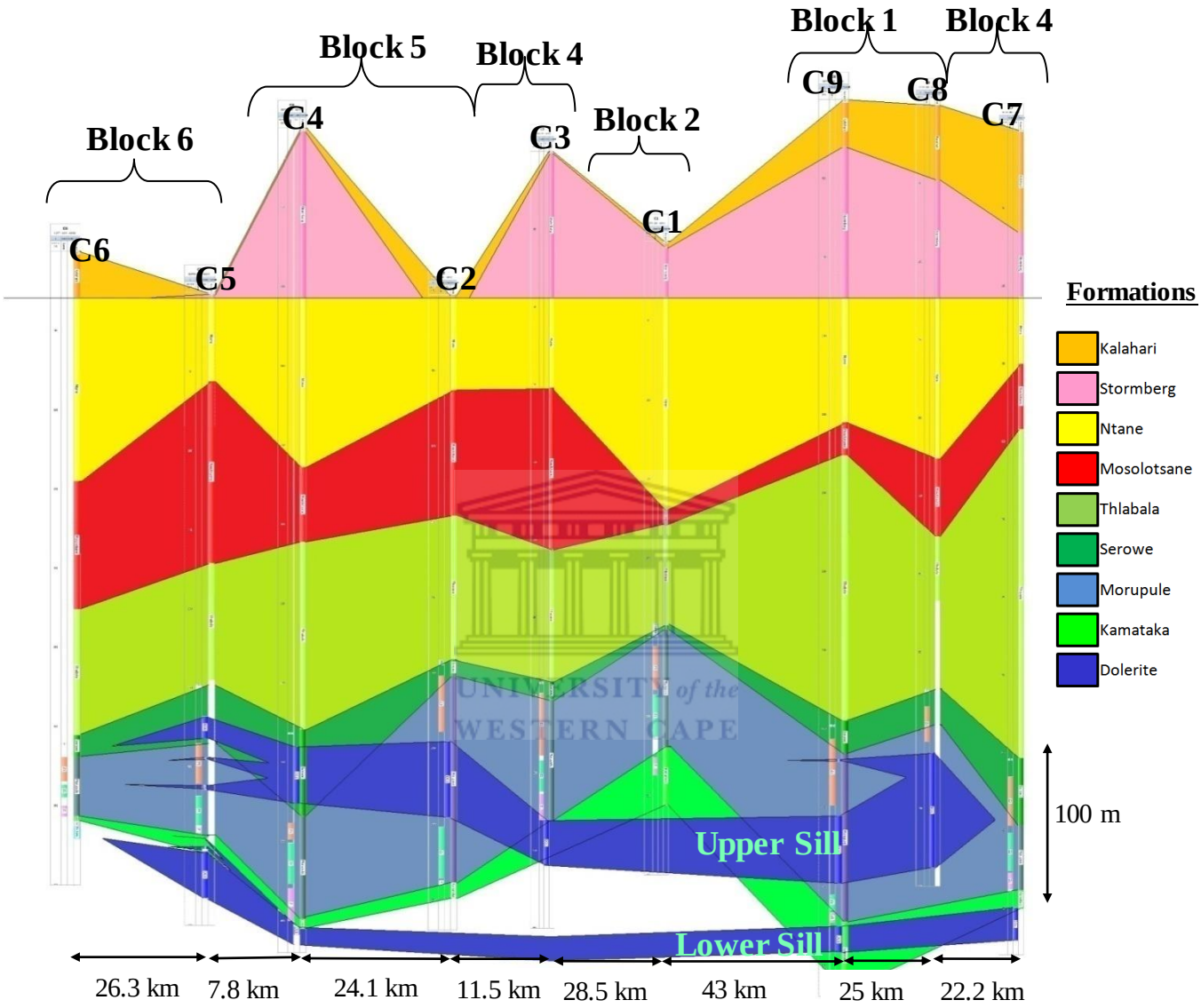

Figure 5.2.1: Cross section encompassing the entire study area, showing the Karoo strata and intrusive dolerite sills.

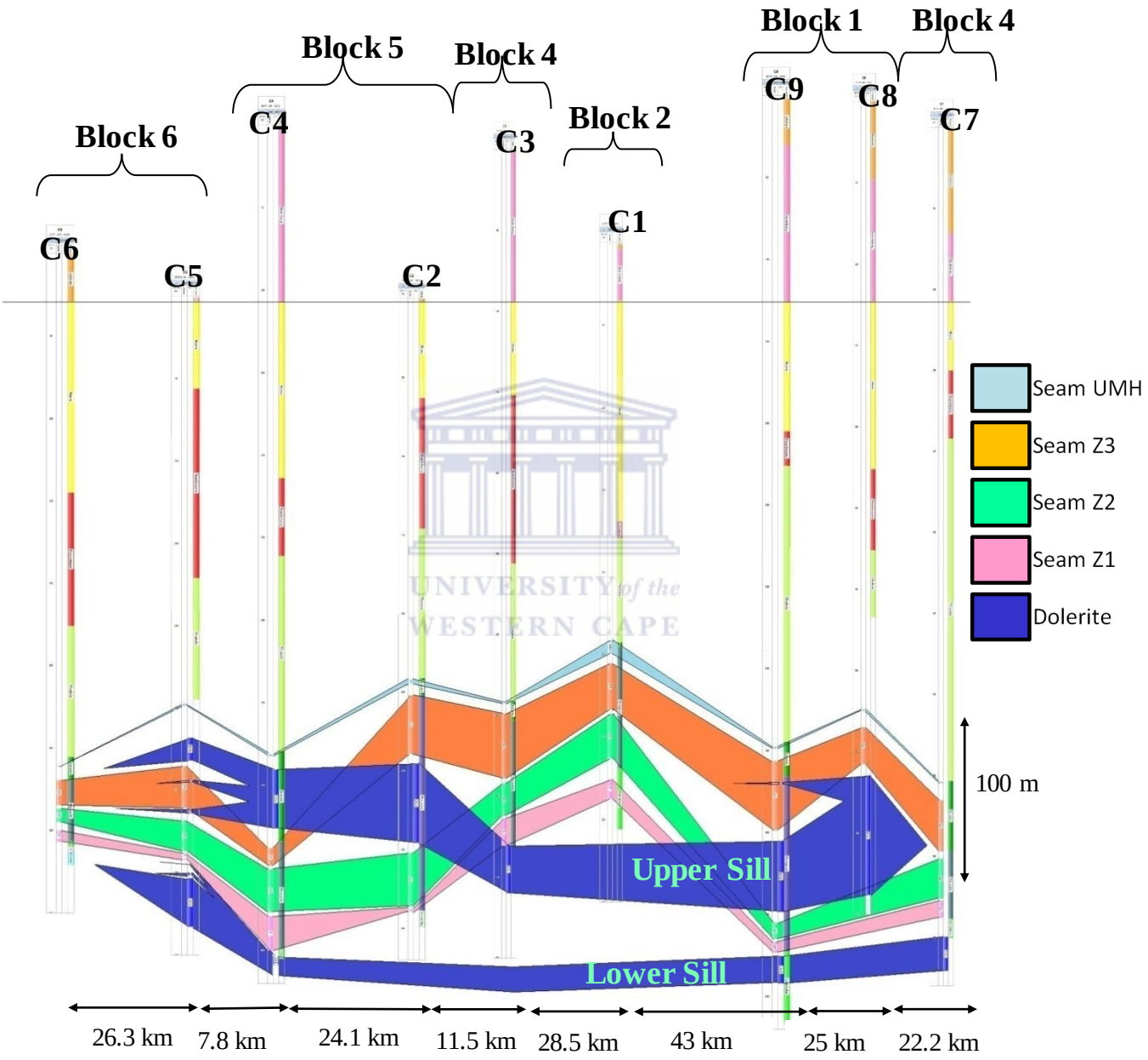

Figure 5.2.2: Interpreted cross section, based on extrapolation, showing the four coal seams and the intruding dolerite sills, which affect boreholes 2, 3, 4, 5, 7, 8 and 9, while boreholes 1 and 6 are dolerite free.

5.2.1 Dolerite Sill Geometry

Previously, the number of dolerite sills in the study area was unknown, but the aeromagnetic data has allowed for the recognition of two sills in the northern part of the study area, which was used as a guide to construct cross sections further south. The cross sections created from the nine log and wireline data have revealed the presence of the two dolerite sills (termed Upper and Lower) throughout most of the study area (Figures 5.2.1 and 5.2.2). Both sills have a standard sill geometry described by Kovac and Cevallos (2012) as well as Galland et al. (2009), with each sill taking on a saucer shape. The base of the saucer is sub-horizontal, and therefore concordant with the intruded strata, while the walls are oblique to the bedding, but which taper and inflect towards concordancy again at their extremities. This can be seen in the section (Figure 5.2.1 as well as Figures B1.7 and B1.8 in Appendix B1) between boreholes C5 and C6, where the topmost finger-like stringer of the upper sill follows the dip angle of the Serowe Formation. Lastly, as proposed by Galland et al. (2009), the lower sill is broader than the upper sill, with not as much flexure in its wall.

5.2.2 Structural Effects of Intrusion

Planar intrusive dolerite sills that are oblique to the Karoo strata cause displacements of marker horizons that can produce various artifacts in the borehole section. These artifacts manifest themselves as changes in apparent thickness of a particular sedimentary horizon, and will be influenced by the pattern of dilation that created the space now occupied by the intrusion. Depending on the location of the borehole relative to the intruded horizon, it is possible to both expand and contract the apparent interval between the top and bottom contacts of the sedimentary unit. If it is assumed that the intrusive sill was emplaced by vertical dilation, then the sedimentary horizon will be apparently “thickened” (or dilated) by the vertical thickness of the intrusion. However, if the sill was emplaced along another axis of dilation, for example orthogonal to the margins of the planar intrusion, a borehole could intersect an apparently condensed (or consumed) section through the sedimentary horizon. An example of apparent dilation can be found in borehole C4, where the Serowe Formation is found to be 54.3 m thick with a 35.5 m thick dolerite intrusion. However, the Serowe Formation in borehole C4 is expected to be only about 18 m thick, maintaining the thickness of the same formation in borehole C2 (of 11m thickness) (Figure 5.2.3).

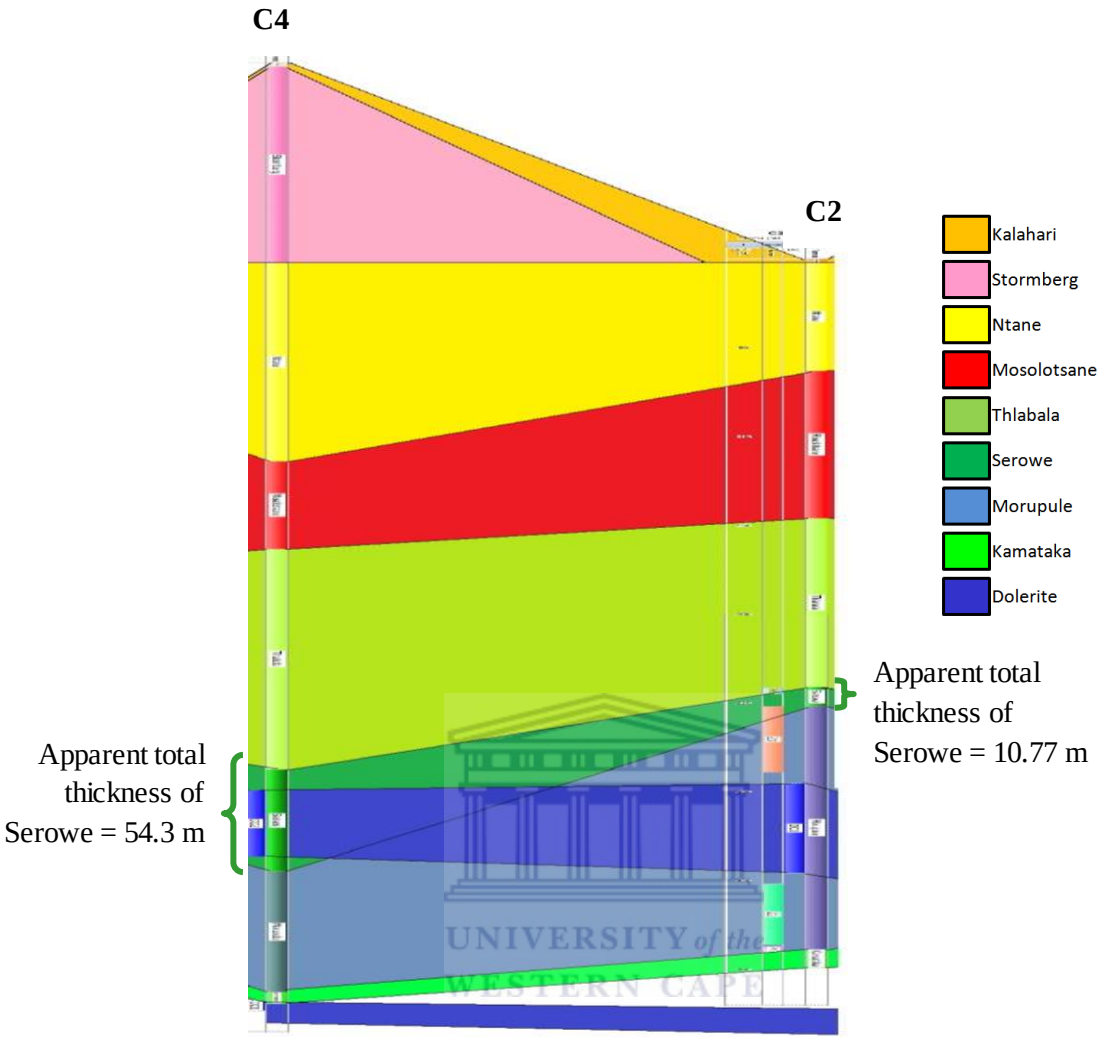

Figure 5.2.3: The thickness of the Serowe Formation in borehole C2 is used as a control in this case as there is no intruding dolerite. The Serowe Formation in the adjacent C4 borehole is a total of 18.81 m thick, with a 35.5 m thick dolerite intrusion. The intrusion is thought to have intruded into the Serowe Formation in borehole C4, along a dilation surface, causing it to have an apparent thickness of 54.3 m.

Conversely, an example of a dolerite sill consuming the host stratigraphy can be seen in the Morupule Formation in borehole C8, where the actual thickness of the Morupule Formation is 17.52 m, which is about 23 m less than expected (Figure B 1.4) once the dolerite thickness has been removed from the calculated thickness. This, compared to the thickness of the same formation in borehole C7, where no dolerite has affected it, shows that the dolerite has consumed at least some of the formation.

Thus, using boreholes C6, C7 and C1as the controls, the other six boreholes that have been affected by the dolerites intruding into the Morupule and Serowe formations, have been assessed, and the results displayed in Tables 5.2.2a and 5.2.2b, with each of the control boreholes being associated with surrounding boreholes. This is achieved by the use of blocks around the associated boreholes in the following two tables. Local topographic variations in thickness should be kept in mind when looking

at whether the formation has been consumed. Borehole C2 can be loosely compared to any of the control boreholes, C1, C6 or C7, as it is far away from all three.

Table 5.2.2a: Effect of dolerite intrusion on the Serowe Formation in each borehole, using the unaffected C1, C6 and C7 boreholes as controls

Borehole	C6	C5	C4	C2	C3	C1	C9	C8	C7
Actual Thickness	13.56m	24.53m	18.81m	10.77m	11.83m	2.48 m	20.85m	23.58m	43.03m
Expected Thickness	13.56m	13.56m	13.56m	13.56m	11.83m	2.48m	20.85m	23.58m	43.03m
Effect of intrusion	None/ Control	Dis-placed	Dis-placed	None	None	None/ Control	None	None	None/ Control

Table 5.2.2b: Effect of dolerite intrusion on the Morupule Formation in each borehole, using the unaffected C1, C6 and C7 boreholes as controls

Borehole	C6	C5	C4	C2	C3	C1	C9	C8	C7
Actual Thickness	37.68m	53.77m	64.85m	88.41m	77.23m	74 m	60.05m	17.52m	42.05m
Expected Thickness	37.68m	37.68m	74 m	74m	74 m	74 m	42.05m	42.05m	42.05m
Effect of intrusion	None/ Control	Diala-ted	Dis-placed	Diala-ted	None	None/ Control	Diala-ted	Cons-umed	None/ Control

A cross section of the four coal seams and dolerite intrusions shows the cross cutting relationship of the dolerite intrusions and coal seams. The cross section shows that the oblique wall of the Upper Sill intrudes across the coal seams, but does not move within the seams themselves, except for the margin of the saucer-shaped sill found in the north at borehole C5 and to the south in borehole C9 in the Z3 coal seam. The Lower Sill is found below the Z1 coal seam of the Morupule Formation, and never intrudes through the seams. The oblique wall of the Lower Sill, however, runs parallel to the bottom of the Z1 seam in the northwestern part of the study area, represented by boreholes C5 and C4. As such, the Z1 coal seam is most likely to have been heat affected in those parts where the Lower Sill comes close to the coal seam, especially towards the edges of the sill.

5.3 Coal Rank

The rank of each coal sample has been determined from the proximate analysis data, as per the criteria outlined in section 4.3, combined with the log data. Examples of these are given in Table 5.3.1 (from borehole C7) and Appendix B3 (boreholes 1-9). The "Comments" column in each of these tables includes comments from the logs and/or core images, and can be used to help determine the coal rank of each sample. The colour coding for each table represents the rank of the coal. In the cases where non-coal data was included in the proximate analysis, actual proximate analysis data was not used, but

the log data and "Comments" can be used to determine if the sedimentary rock has been affected by the intrusion.

Table 5.3.1: Proximate data of coal samples taken from borehole C7. Tables for the other boreholes can be found in Appendix B3.The proximate analysis data have been interpreted to determine the rank of coal. Included is the depth of the dolerite sills, and extra comments from the log data. The various colours indicate the various ranks of the coal: Orange = Anthracite; yellow= metasomatised; light green= bituminous coal; light blue = sub-bituminous coal; bright green= non-coal samples.

Sample Number	Formation	Top Depth	Bottom Depth	Moisture	Ash	Volatile Matter	Fixed Carbon	Seam	Rank	Comments
		(m)	(m)	(%)	(%)	(%)	(%)			
1G	Serowe	403.47	403.83	6.21	43.71	25.56	24.52		Meta	Highly fractured
2G	Serowe	403.83	404.43	6.36	29.78	32.85	31.01	UMH	Subbit	Calcite in fractures
3G	Serowe	415.22	415.82	5.15	39.33	23.80	31.73	Z3	Devol	Siderite is common
4G	Serowe	416.70	417.30	5.89	31.74	25.30	37.08	Z3	Subbit	Abundand siderite
5G	Serowe	417.30	417.90	6.48	15.09	32.00	46.43	Z3	Subbit	Abundand siderite
6G	Serowe	418.04	418.47	5.42	21.52	29.44	43.63	Z3	Subbit	Abundand siderite
7G	Serowe	418.87	419.25	4.09	39.78	31.26	24.86	Z3	Non-coal	Mudstone and coal
8G	Serowe	423.08	423.68	4.77	14.42	33.49	47.32	Z3	Subbit	Siderite present
9G	Serowe	423.68	424.28	5.05	15.23	33.64	46.08	Z3	Subbit	Siderite present
10G	Serowe	428.23	428.72	3.91	31.31	32.09	32.70	Z3	Subbit	Siderite present
11G	Serowe	432.36	432.96	4.78	13.91	33.51	47.81	Z3	Subbit	Siderite present
12G	Serowe	432.96	433.56	4.09	17.17	31.58	47.17	Z3	Subbit	Siderite present
13G	Serowe	433.92	434.52	3.79	22.26	30.01	43.94	Z3	Subbit	Siderite present
14G	Serowe	438.75	439.35	3.67	20.70	30.39	45.24	Z3	Subbit	Siderite present
15G	Serowe	439.35	439.95	3.84	13.30	35.68	47.18	Z3	Subbit	Siderite present
16G	Serowe	439.95	440.55	3.52	22.65	28.88	44.95	Z3	Subbit	Siderite present
17G	Morupule	451.38	451.75	2.89	29.19	34.14	33.78	Z2	Subbit	Abundand siderite
18G	Morupule	456.37	456.93	3.65	19.86	32.31	44.19	Z2	Subbit	Siderite present
19G	Morupule	456.93	457.50	3.11	27.09	34.23	35.58	Z2	Subbit	Siderite present
20G	Morupule	460.24	460.70	3.58	23.72	31.11	41.59	Z2	Subbit	Siderite present
21G	Morupule	462.86	463.14	3.72	12.91	32.05	51.33	Z2	Bit	Siderite present
22G	Morupule	469.69	470.29	2.65	37.57	31.34	28.44	Z2	Devol	Clean fractures
23G	Morupule	473.55	474.15	3.44	36.34	17.73	42.50	Z2	Devol	Clean fractures
24G	Morupule	481.69	482.29	1.61	25.56	16.50	56.33	Z1	Bit	Clean fractures
25G	Morupule	485.62	486.22	1.30	22.10	9.42	67.18	Z1	Devol	Calcite in fractures
Dolerite at 499.54 - 520.79 m										

Note: The proximate data for each sample has been interpreted to determine the rank of coal. Included is the depth of the dolerite sills, and extra comments from the log data. The various colours indicate the various ranks of the coal: Orange = Anthracite; yellow= metasomatised; light green= bituminous coal; light blue = sub-bituminous coal; bright green= non-coal samples.

Most of the coal, despite the seam to which it belongs, has been classified as sub-bituminous ("Subbit", highlighted in light blue in Table 6), using the approach of Bennett (1989), as well as the

proximate analysis data. This can be seen in the proximate analysis for boreholes C1 and C6 (Appendix B3), where no dolerite intrusions were intercepted, and so were used as a control. The "devolatilised" zones were determined by an ash content of greater than 36 wt. % (Sasol, 2011), or the log classifies them as "burned", "devolatilised", or "baked". These zones occur stratigraphically close to the dolerite intrusion, as with samples 22G, 23G and 25G in borehole C7 (Table 6). In these cases, the dolerite has intruded close to, or adjacent to the coal, causing the coal to burn and become devolatilised. In other cases, the dolerite has intruded far enough from the coal to not burn it, but to cause it to increase in rank from sub-bituminous to bituminous, due to thermal effects, thereby increasing the fixed carbon content, causing an associated, relative decrease in the ash, volatile matter and moisture content, e.g. samples 21G and 24G in borehole C7 (Table 6). In the case of samples D19 and D20 from borehole C4, the dolerite intrusion has increased the coal rank from the original sub-bituminous coal to anthracite, where the vitrinite reflectance is visible, according to the log data, and the coal is bright, as opposed to dull. In this case, the dolerite has caused the fixed carbon content to increase to greater than 70 wt.%. But this effect is only restricted to a small scale, where only the nearby coal (up to 30 m above or below the intrusion) was affected.

Another way in which the dolerite has affected the coal is by metasomatism. It has been proposed that the heat of the intrusion causes the water and other fluids, such as gaseous carbon, from the country rock to be released through mineral dehydration, oxidation and kerogen cracking to methane (Figure 5.3.1) (Aarnes et al., 2010; Bussio, 2012). Subsequent migration of these fluids could extend beyond the zone affected by simple thermal conduction, thereby causing a metasomatic effect that manifests to a larger scale. In the study area, this has been identified in samples with a high ash content (greater than 36 wt.% due to the presence of siderite and calcite caused by fluid movement) that do not occur stratigraphically close to a dolerite intrusion, as with sample 1G in borehole C7 (Table 5.3.1). The mobile fluid moves away from the heat source through the fractures present in the coal dissolving out the volatiles present in the coal, and allowing for other minerals, such as calcite, to precipitate.

With the possibility of wide scale metasomatism in mind, the log was then used to identify samples that had calcite present in fractures, cleats and veins. In most cases these were found to be minor, but in some cases, the effect was enough to cause the volatile content to decrease, thereby dramatically increasing the ash content, as in samples D001, D002 and D005 from borehole C6. It is evident, from the logs that borehole C6 did not intercept any dolerite sill or dyke, and so should have coals ranked as sub-bituminous to bituminous, with an ash content of less than 20 wt.%. This is not so in the metasomatised samples. Also, the log data and core images (Figure 5.3.2) show that the core sample is highly fractured, and contains calcite in the cleats.

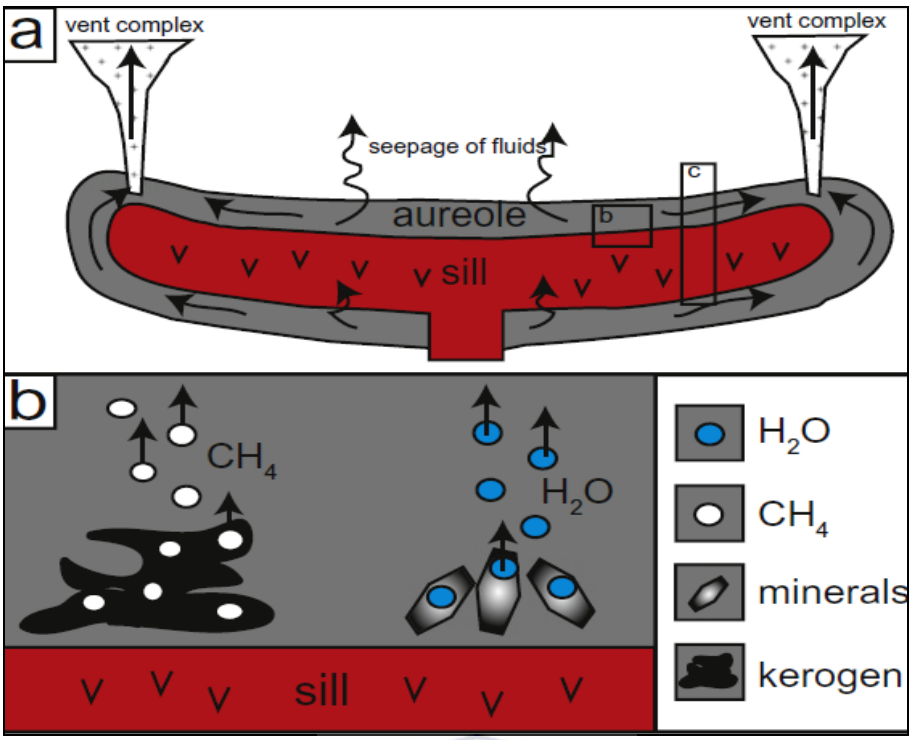

Figure 5.3.1: a) An emplaced sill forms a thermal aureole in the surrounding country rock, and overpressure may cause vent complexes to form. b) The heat of the intrusion causes kerogen to crack to methane, and, other minerals to dehydrate as they prograde, thereby releasing H_2O, which becomes mobile in the surrounding country rock due to the increased temperatures and pressures. From: Aarnes et al. (2010)

Figure 5.3.2: Sample D001 fromborehole C6 (319.04 - 319.59 m depth), showing a zone of fracturing with calcite precipitation. This zone is interpreted as being the result of metasomatism caused by the movement of mobile fluids through the system.(Image supplied by Kubu Energy).

Golab and Carr (2004) suggested that the presence of siderite indicates that a bituminous or sub-bituminous coal has been thermally affected, and also metasomatised by an intrusion. The log data supplied for each of the nine boreholes shows that much of the bituminous and sub-bituminous coal does indeed contain siderite (Table 6; Appendix B3). The presence of the siderite increases the ash content, and, if found within cleats and fractures, decreases the permeability of the coals.

5.4 Effects of Dolerite Sills on Coal

Dolerite sills can locally increase the temperature of the coal-bearing strata through thermal conduction. Within this thermal aureole the coal can combust if near the contact, depending on the size of the intrusion, but elsewhere the rank of the coal can be increased. According to Johnson et al. (1963) a less rapid heating, or an increase in pressure on the coal will lead to an increase in coal rank, whereas a rapid heating will cause it to burn or devolatilise. The anthracite that formed in borehole C7(samples D19 and D20 – Table 6) was due to a pressure increase acting on the resident sub-bituminous ranked coal. Al-Jubori et al. (2009) noted that the higher the coal rank, the higher the volume of gas adsorbed onto the coal surface (Figure 5.4.1).

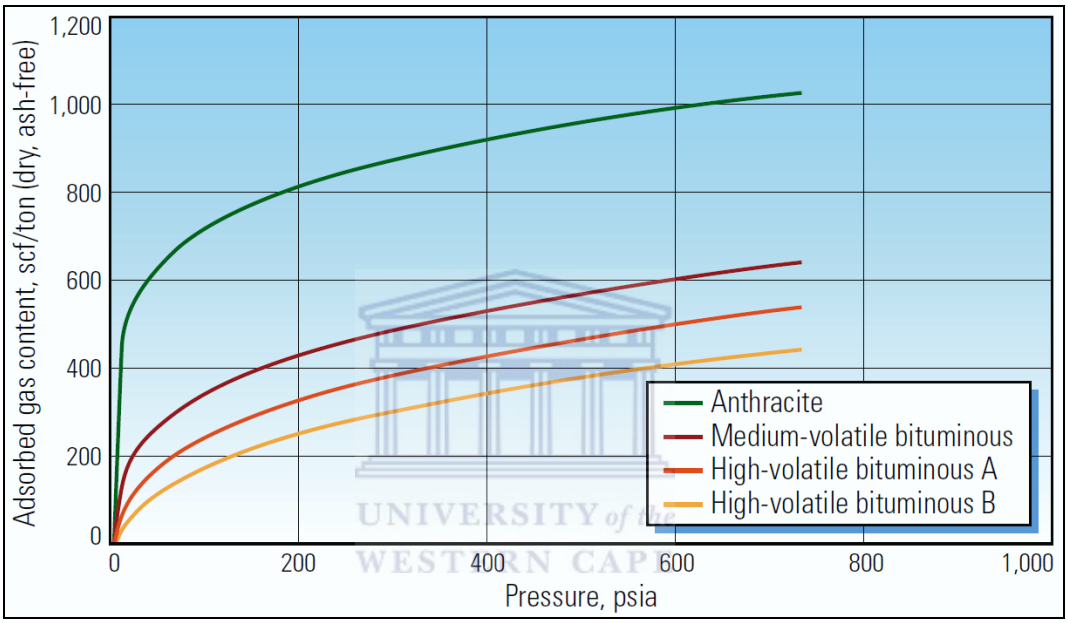

Figure 5.4.1: Relationship between adsorbed gas and confining pressure. A higher rank coal allows more gas (mainly methane) to be adsorbed onto its surface. Bituminous coal is represented by the yellow, orange and red lines, each of which is a higher sub-rank than the last. From: Al-Jubori et al. (2009).

Even though anthracite has a higher adsorbed gas content as opposed to other coal ranks (Al-Jubori et al, 2009), the pressure at which it forms is too high to maintain a cleat or fracture system of a viable CBM reservoir.

Metasomatism of coal has the potential of generating an affected zone on a larger scale than that of direct heat effects, as released fluids can migrate beyond the thermal aureole (Aarnes et al., 2010; Bussio, 2012). As the fluids move through the coal and surrounding country rock, the volatiles are dissolved out of the coal and into the fluids, where they are carried away by the fluids. This decreases the quality of the coal by removing the methane, and increasing the ash content, due to the precipitation of secondary mineral veins and pores, such as calcite, which clog fractures, cleats ad macropores in the coal reducing the permeability of an already tight reservoir, and counteracting the effects of coal rank, which may have increased due to the heat applied by the intrusion.

6. Conclusions

The Permian Ecca Group in Southern Africa was deposited before the breakup of the Gondwana Supercontinent (Catuneanu et al., 2005). The breakup of the supercontinent caused the extrusion of the Drakensberg Lava Group and the intrusion of the Karoo dolerites into the existing strata, exploiting the pre-existing SE-NW fault systems, at 180 Ma. The two saucer shaped Karoo dolerite sills found in the study area, referred to as the Upper and Lower Sills, were initially noted in the aeromagnetic data. The log data, of the study area, shows the lateral continuity of these sills to the southern part of the study area.

The cross sections created from the log data show that the Upper Sill has intruded into the Serowe and Morupule Formations, along dilation planes, with the base and extremities of the sill concordant with the country rock strata, while its walls cut obliquely across the country rock (Figure B1.7). The Lower Sill is located in the lower Ecca Group (Kamataka Formation), with the walls and extremities intruding only to the base of the Morupule Formation (Figure B1.7). In this case, on a small scale the Upper Sill has thermally affected the Serowe and Upper Morupule Formation coals, while the Lower Sill has thermally affected the lower Morupule Formation coals.

One of the ways the intruded dolerite sills have affected the coal seams is by either displacing/ dilating or by consuming/removing the coal. In most cases, the dolerite sills have dilated the country rock, causing an apparent increase in thickness of the affected formation. The oblique areas of the sills, especially those of the Upper Sill, have consumed the coal. An example where coal has been consumed can be found in the area between boreholes C2 and C3 (Figure B1.7). This dilation vs. consumption of the intruded country rock depends on the axis of dilation when the dolerite intrudes.

The dolerite intrusions have also affected the coal thermally. The heat given off from the intrusions is dependent on the distance travelled, density, and temperature of the intrusion (Bussio, 2012), along with a few other lesser factors. The sudden increase in heat given off to the country rock during the intrusion of the dolerite sills has caused the nearby coals (up to 30 m away) to be burned and thus devolatilised. These coals are defined by an ash content of more than 36 wt.% in the proximate analysis. The bituminous and sub-bituminous coals that are much further away from the intrusions can easily be classified as “heat affected” by the presence of siderite (Golab and Carr, 2004), which forms due to diagenetic processes that occur at higher temperatures, which cause a sub-bituminous, or even bituminous coal to become heat affected. The presence of the siderite causes an increase in the ash content, and, although the coal rank remains unchanged, and the coal is not devolatilised, the coal quality is decreased, and may not be viable for CBM extraction.

A third way in which the dolerite intrusions have affected the coal is by increasing the coal rank. This is due to an increase in temperature, as well as pressure, that is brought about by an intrusion. The coal found in Botswana, and the study area, is mainly sub-bituminous and bituminous. In this study area, the dolerite sills have caused some of those sub-bituminous coals to increase in rank to bituminous and anthracite. An example is seen in the proxy data for samples D19 and D20 from borehole C4, where the coal has been ranked as anthracite. In the case of Coalbed methane mining, the upgrade tin rank from sub-bituminous to bituminous is a good thing, baring the presence of siderite, as the cleat system has not been affected directly by the heat. However, an upgrade to an anthracitic coal has a negative effect on CBM, as a localized increase in pressure causes the cleat system to close, thereby further reducing the permeability of the reservoir.

The fourth and last effect of the dolerite sills mentioned in this study is metasomatism. This is caused by fluids from the country rock that becomes mobile due to the increase in temperature due to the intrusion of the sill(s). These fluids move through the cleat and fracture systems dissolving out the volatile matter (usually methane) from the coal, and allowing for the precipitation of calcite and other minerals. These precipitated minerals have two major negative effects on the coal, the first is that they act as a cement within the cleat system, thereby reducing the permeability within the reservoir, and, secondly, it increases the ash content of the coal by the addition of non-coal material. Both of these effects are far reaching, as the fluids are very mobile and so affect the coal on a larger scale than the thermal effects of the intrusions do.

On the whole, the two dolerite sills that have been emplaced into the Karoo Supergroup strata in the study area have far reaching effects. Coalbed methane extraction requires thick bituminous coal seams, that are not heat affected. It is not recommended that the current license blocks A, B and C be pursued further, as the coal in this area has been badly heat affected as well as metasomatised by the two intruding sills in the area.

Looking at the regional geology, it is recommended that if a CBM project is being sought in Botswana, the Central Kalahari sub-basin is surely the basin to prove successful. However, a location further south, away from the Okavango Dyke Swarm is recommended (Figure 2.1.1), where there are not as many feeder dykes to potential dolerite sills. The Passarge and Nosob Ncojane sag basins located on the western part of the Kalahari sub-basin are not recommended as potential target areas, as the coal in these sag basins have been buried to depths greater than 1000 m, causing excessive pressures in the coal, which would negatively affect the cleat system, and thus the permeability of the coal. Also, the coal being buried to these great depths would most likely cause it to metamorphose to anthracite, which is not viable for CBM.

The limited data available in this project does not allow for much more recommendations to be made, other than to suggest that should further investigation into the CBM potential of blocks A, B and C

continue, the reservoir quality of the coal should be evaluated, taking into account the altered state of the coals.

7. References

Aarnes, I., Svensen, H., Connolly, J.A.D., Podladchikov, Y.Y. 2010. How contact metamorphism can trigger global climate changes: Modeling gas generation around igneous sills in sedimentary basins. *Geochimicael Cosmochima Acta*, **74**:7179-7195.

Al-Jubori, A., Johnston, S., Boyer, C., Lambert, S.W., Bustos, O.A., Pashin, J.C., Wray, A. 2009. Coalbed Methane: Clean Energy for the World. *Oilfield Review*, **21**(2): 4-13.

Aminian, K. 2005. Coalbed Methane-Fundamental Concepts, Technical report, Petroleum and Natural Gas Engineering Department, West Virginia University.

ARI. 2003. Results of the Central Kalahari Karoo Basin Coalbed Methane Feasibility Study, prepared for the Department of Geologic Survey, Botswana, Lobatse.

Bennett, J.D., 1989. Review of Lower Karoo coal basins and coal resource development in parts of central and southern Africa with particular reference to northern Malawi. *Technical Report WC/89/21 British Geological Survey.*

Boggs, S. Jr. 2010. *Principles of sedimentology and stratigraphy*, 4th edn., Pearson Education International, University of Oregon

Bordy, E.M., Segwabe, T., Makuke, B., 2010.Sedimentology of the Upper Triassic-Lower Jurassic (?)Mosolotsane Formation (Karoo Supergroup), Kalahari Karoo Basin, Botswana.*Journal of African Earth Sciences*, **58**: 127-140.

Bussio, J.P., 2012. *Effect of dolerite intrusions on coal quality in the Secunda Coal Fields of South Africa*.Pretoria: University of Pretoria. (MSc thesis)

Catuneanu, O., Wopfner, H., Eriksson, P.G., Cairncross, B., Rubidge, B.S., Smith, R.M.H., Hancox., P.J. 2005, The Karoo basins of south-central Africa. *Journal of African Earth Sciences*, **43**:211-253.

DeCelles, P.G. and Giles, K.A., 1996. Foreland basin systems, *Basin Research*, **8**: 105-123.

Elburg, M., Goldberg, A., 2000. Age and geochemistry of Karoo dolerite dykes from northeast Botswana, *Journal of African Earth Sciences*, **31** (3/4): 539-554

Galland, O., Planke, S., Neumann, E.R., Sorenssen, A.M. 2009. Experimental modeling of shallow magma emplacement: Application to saucer-shaped intrusions. *Earth and Planetary Science Letters*, **277**:373-383.

Geological Survey and Mines Department, 1973. Botswana. *Geological Map of Botswana*, 1:1 000 000, Lobatse: Geological Survey and Mines Department

Global Methane Initiative, 2010. Coal Mine Methane Country Profiles. Prepared by U.S, Environmental Protection Agency Coalbed Methane Outreach Programme, pp. 21-25.

Golab, A.N., Carr, P.F., 2004. Changes in geochemistry and mineralogy of thermally altered coal, Upper Hunter Valley, Australia. *International Journey of Coal Geology* **57,** (3-4):197-210.

Haddon, I.G., 2005. *The sub-Kalahari geology and tectonic evolution of the Kalahari Basin, Southern Africa*.Johannesburg: University of the Witwatersrand. (PhD Thesis)

Haddon, I.G., McCarthy, T.S. 2005. The Mesozoic-Cenozoic interior sag basins of Central Africa: The Late-Cretaceous – Cenozoic Kalahari and Okavango basins. *Journal of African Earth Sciences*, **43**: 316-333.

Halliburton, 2008.Coalbed Methane: Principles and Practices. Accessed from: http://www.halliburton.com/public/pe/contents/Books_and_Catalogs/web/CBM/CBM_Book_Intro.pdf; accessed on: 12 November 2013

James, D.E., Niu, F., Rokosky, J. 2003. Crustal structure of the Kaapvaal craton and its significance for early crustal evolution. *Lithos*, **71** (2003): 413-429

Johnson, V.H., Gray, R.J., Schapiro, N. 1963. Effect of Igneous intrusives on the chemical, physical, and optical properties of Somerset Coal. *ENFL*, 7(2):110-124

Jourdan, F., Feraud, G., Bertrand, H., Kampunzu, A.B., Tshoso, G., Le Gall, B., Tiercelin, J.J., Capiez, P. 2004. The Karoo triple junction questioned: evidence from Jurassic and Proterozoic $^{40}Ar/^{39}Ar$ ages and geochemistry of the giant Okavango dyke swarm (Botswana). *Earth and Planetary Science Letters*, **222** (2004): 989-1006

Kovac, P., Cevallos, C. 2012, Airborne Magnetic Data Acquisition Botswana Coalbed Methane Project. Technical Report on Geological Interpretation of Airborne Magnetic Data.Unpublished. Prepared by: Fugro Airborne Surveys Pty. Ltd., for Sasol Petroleum Botswana

Le Gall, B., Tshoso, G., Jourdan, F., Feraud, G., Bertrand, H., Tiercelin, J.J., Kampunzu, A.B., Modisi, M.P., Dyment, J., Maia, M. 2002. $^{40}Ar/^{39}Ar$ geochronology and structural data from the giant Okavango and related mafic dyke swarms, Karoo igneous province, northern Botswana. *Earth and Planetary Science Letters*, **202**: 595-606

Le Gall, B., Tshoso, G., Dyment, J., Kampunzu, A. B., Jourdan, F., Feraud, G., Bertrand., H., Aubourg, C., Vetel, W. 2005. Okavango giant mafic dyke swarm (NE Botswana): its structural significance within the Karoo Large Igneous Province. *Journal of Structural Geology*, **27** (2005): 2234-2255

Modie, B.N. 2007.*Palaeozoicpalynostratrigraphy of the Karoo Supergroup and palynofacies insight into palaeoenvironmental interpretations, Kalahari Karoo Basin, Botswana*. Université de Bretagne Occidentale. (PhD Thesis)

Potgieter, J., 2012. Botswana CBM: Botswana Exploration Corehole Project, Detailed Operating Plan: Wireline Logging. *Unpublished*

Potgieter, J., Anderson, N. 2012. An evaluation of the coalbed methane potential of the central Kalahari area of Botswana from a geological perspective.*Unpublished*. Prepared for: Kubu Energy Resources

Sasol, 2011, Sasol, viewed 07 August 2013, <http://www.sasol.com/media-centre/media-releases/sasol-announces-joint-venture-participation-origin-energy-coal-bed>.

Scheffler, K., Buehmann, D., Schwark, L. 2006. Analysis of late Paleozoic glacial to postglacial sedimentary successions in South Africa by geochemical proxies – Response to climate evolution and sedimentary environment. *Palaeogeography, Palaeoclimatology, Palaeoecology*, **240** (2006): 184-203

Segwabe, T., 2008.*The Geological Framework and Depositional Environments of the Coal-Bearing Karoo Strata in the Central Kalahari Karoo Basin, Botswana.* Rhodes University.(MSc Thesis)

Smith, R.A. 1984. The lithostratigraphy of the Karoo Supergroup in Botswana: A Report on the geophysical and geological results of follow-up drilling to the Aeromagnetic Survey of Botswana. *Geological Survey Department*. Bulletin 26, Lobatse, Botswana

Speight, G. 2005. 'Handbook of Coal Analysis' in J.D. Winefordner (Ed.), Chemical Analysis: A Series of Monographs on Analytical Chemistry and its Applications, v. 166, Wiley-Interscience, New-Jersey

Visser, J.N.J. 1995. Post-glacial Permian stratigraphy and geography of southern and central Africa: boundary conditions for climatic modeling. *Palaeogeography, Palaeoclimatology, Palaeoecology* **118** (1995): 213-243

White, C.M., Smith, D.H., Jones, K.L., Goodman, A.L., Jikich, S.A., LaCount, R.B., DuBose, S.B., Ozdemir, E., Morsi, B.I., Schroeder, K.T. 2005. Sequestration of Carbon Dioxide in Coal with Enhanced Coalbed Methane Recovery – A Review. *Energy Fuels*, **19** (3): 659- 724

Zhou, 2012. The SADC Regional Infrastructure Development Master Plan- Energy Sector Plan prepared by EECG Consultants Pty. Ltd. for: Southern African Development Community Secretariat

Appendix A: Data Provided

A1. Interpreted Aeromagnetic Map

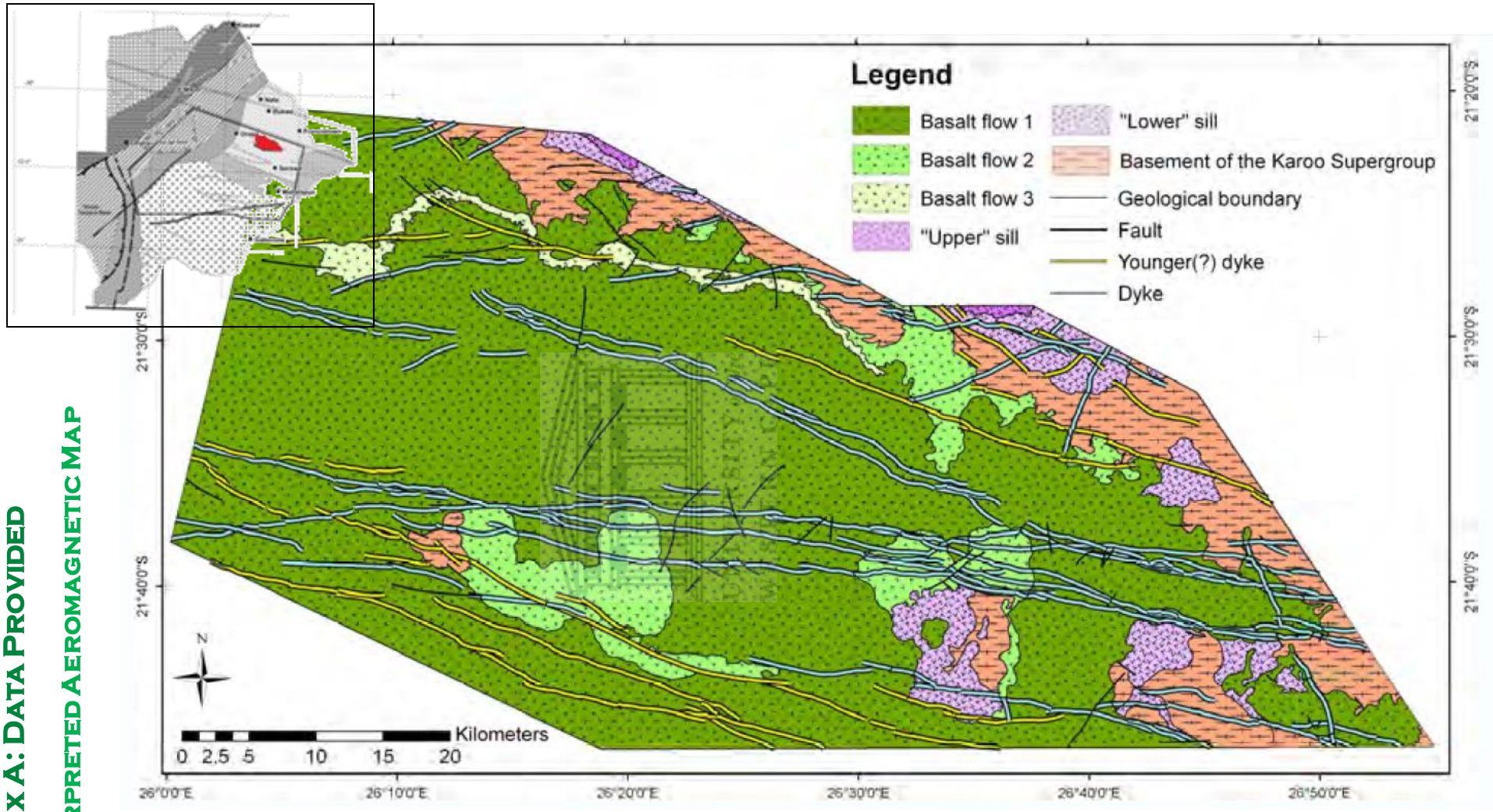

Figure A1: The interpreted aeromagnetic map over the study area, showing the basalt flows (greens), dolerite sils (purples), basement (peach), dykes (blue and yellow lines) and faults (black lines). The Karoo Supergroup is not magnetically visible, and so does not show up on the magnetic map. From: Kovac and Cevallos (2012).

A2. Core images

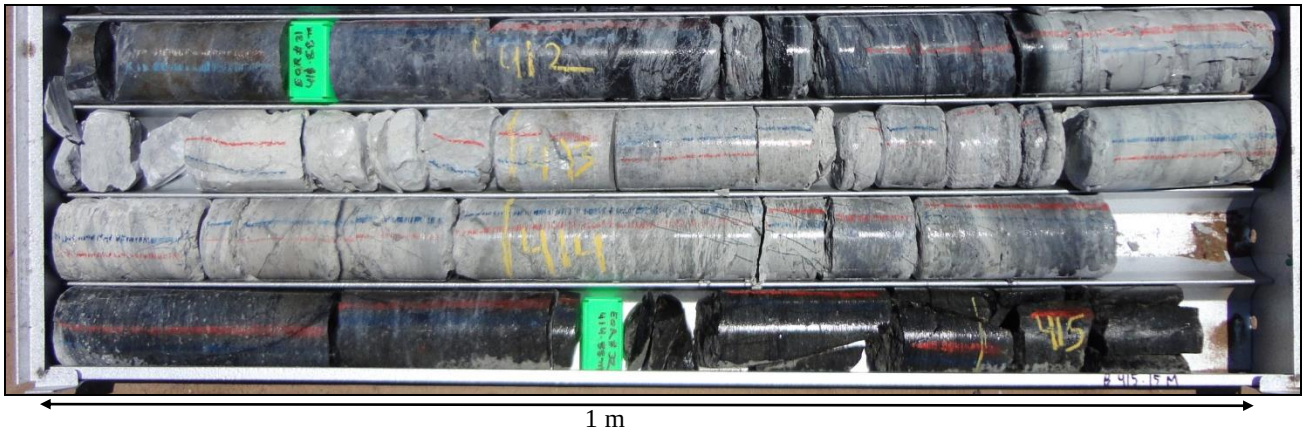

Figure A2.1: Baked mudstone, shown here from a depth of 411.67 m to 414.51 m from borehole C7, directly in contact with a darker dolerite. The heat from the dolerite has affected the overlying mudstone at depths as shallow as 409 m deep, causing it to take on a lighter shade.

A3. Proximate Analysis Samples

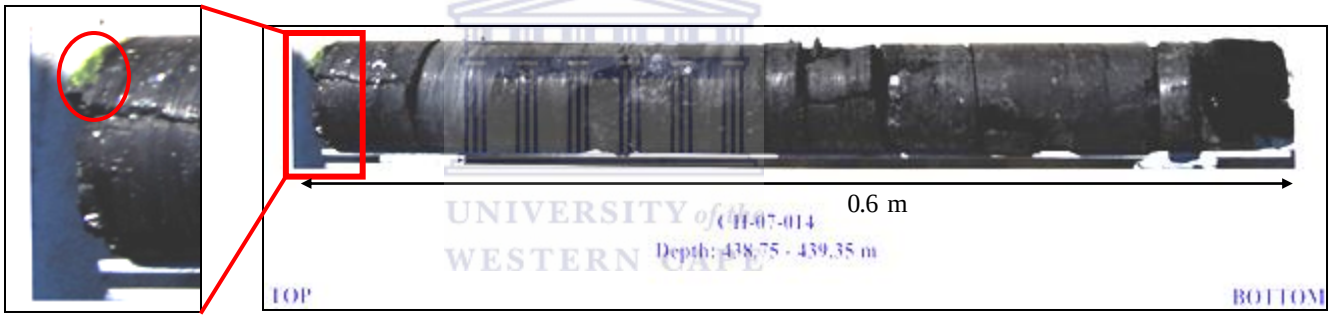

Figure A3.1: Sub-bituminous coal sample from borehole C7, at a depth of 438.75 - 439.35 m. The sub-bituminous coal is a dark grey to black colour. The presence of green siderite is evident at the very top of this sample, and indicated in the magnified image.

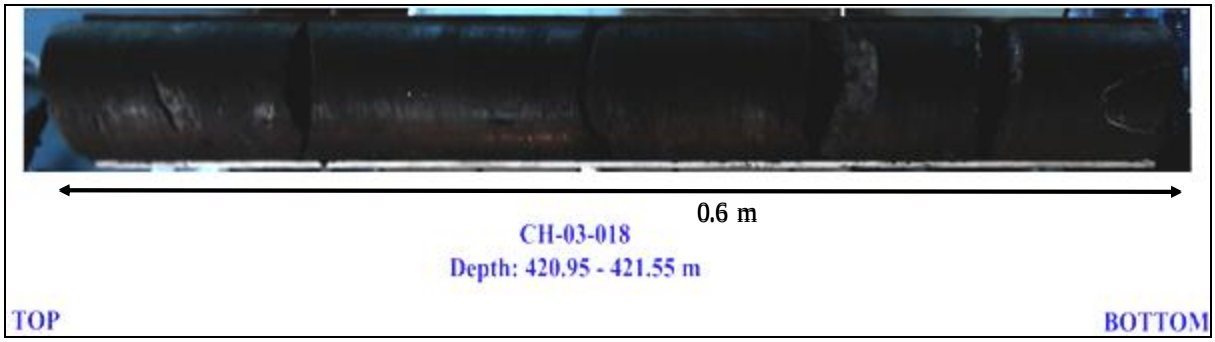

Figure A3.2: A bituminous coal sample from borehole C3, at a depth of 420.95 - 421.55 m. The coal sample has a brown-black hue, and is quite dark.

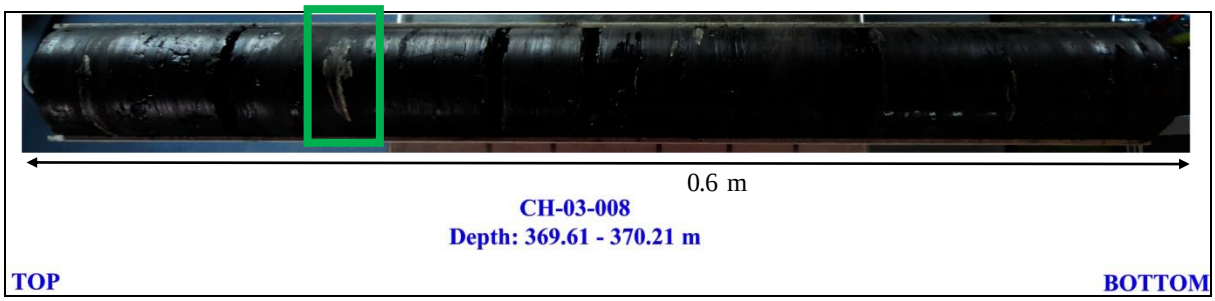

Figure A3.3: A metasomatised sample taken from borehole C3, at a depth of 369.61 - 370.21 m. The sample looks like a standard bituminous or sub-bituminous sample, except for its highly fractured nature, and presence of calcite that has precipitated in the fracture, (shown within the green box).

Figure A3.4: Devolatilised coal appears to be burned and takes on a lighter hue; just as burned mudstone does in Figure A2.1 in Appendix A. This sample has been taken from borehole C7 at a depth of 473.55 – 474.15 m.

Appendix B: Interpretation

B 1 . Cross Sections- Dolerite and Formations

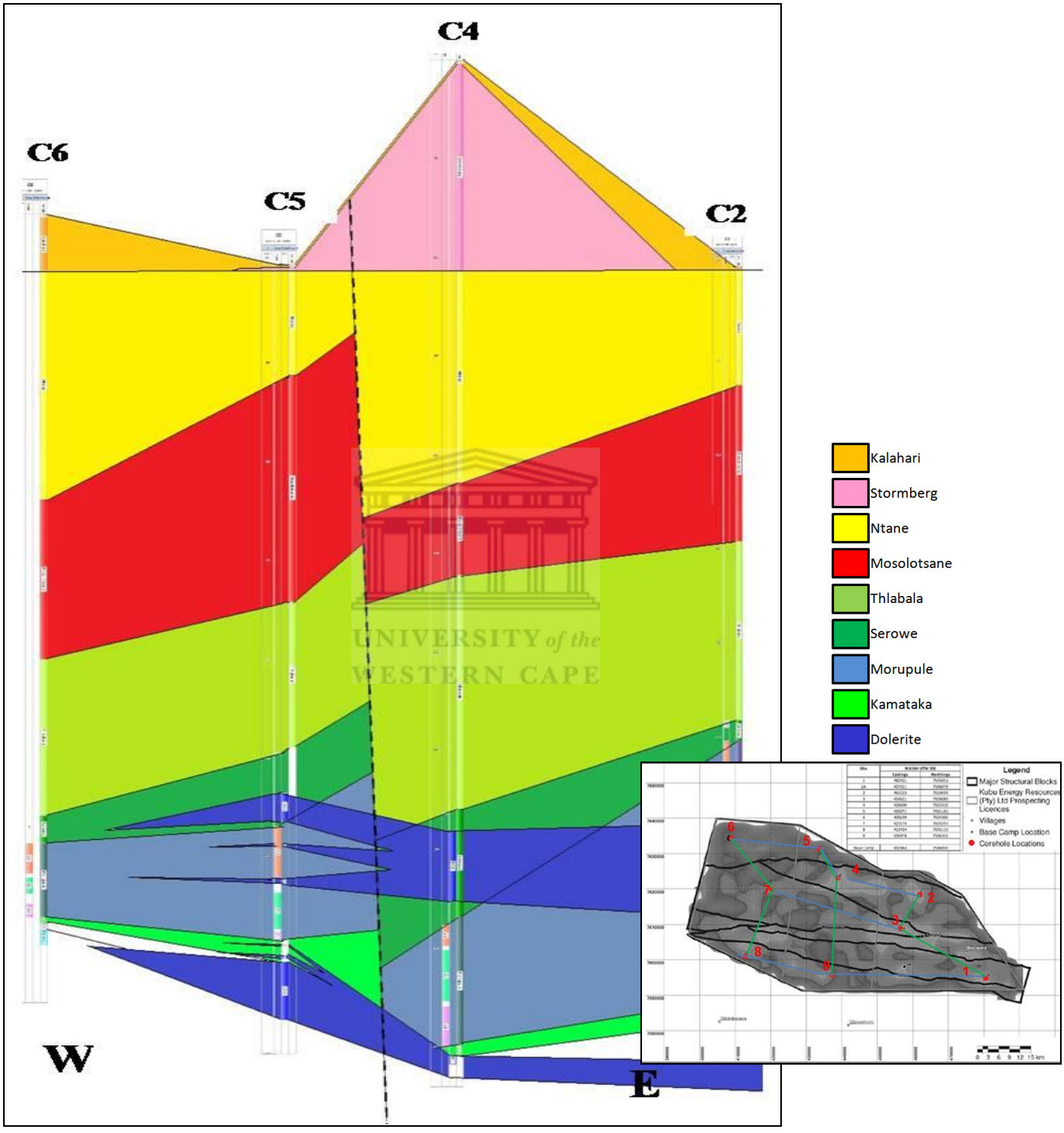

Figure B1.1: An approximate west-east cross section interpreted using the logs provided by Kubu Energy for boreholes C6, C5, C4 and C2, crossing the northern portion of the study area. The fault line (f) indicates an area of major throw located between boreholes C5 and C4, which can also be seen in the aeromagnetic data (Figure 4.2.1). The legend in this figure applies to all the figures in Appendix B1.

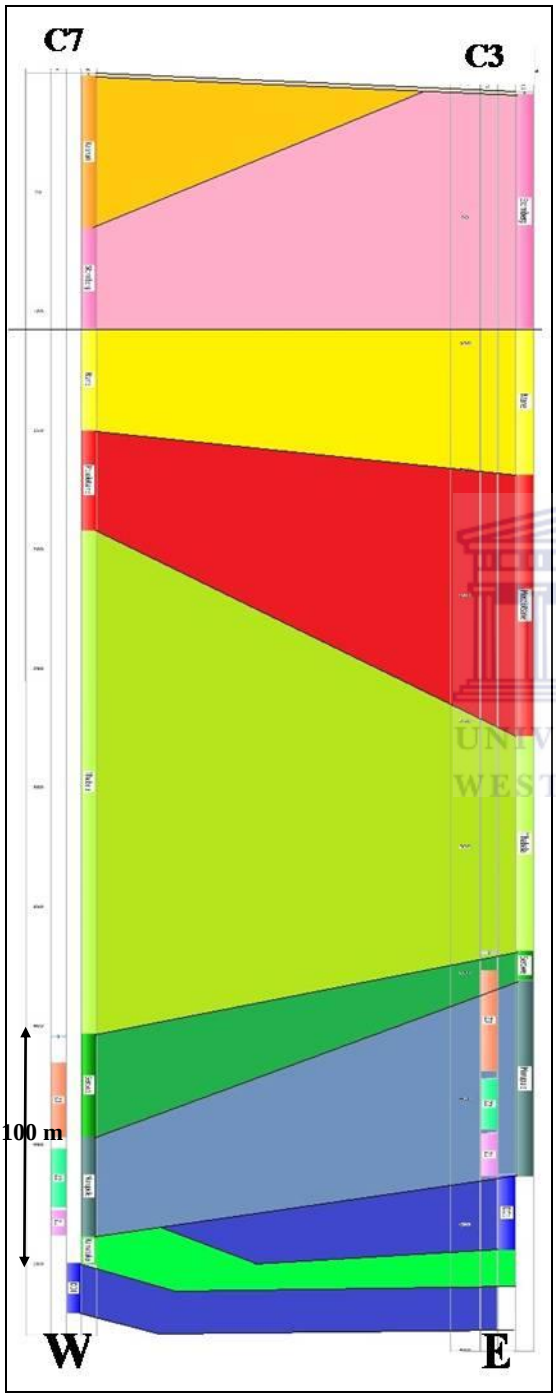

Figure B1.2: An approximate west-east cross section interpreted using logs provided for boreholes C7 and C3, crossing the central part of the study area.

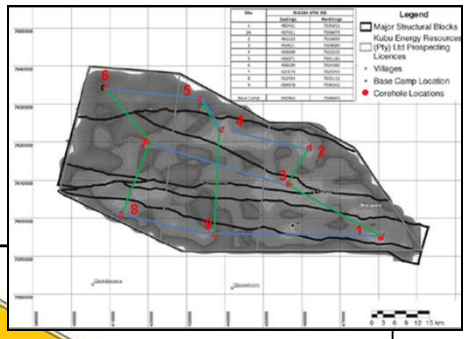

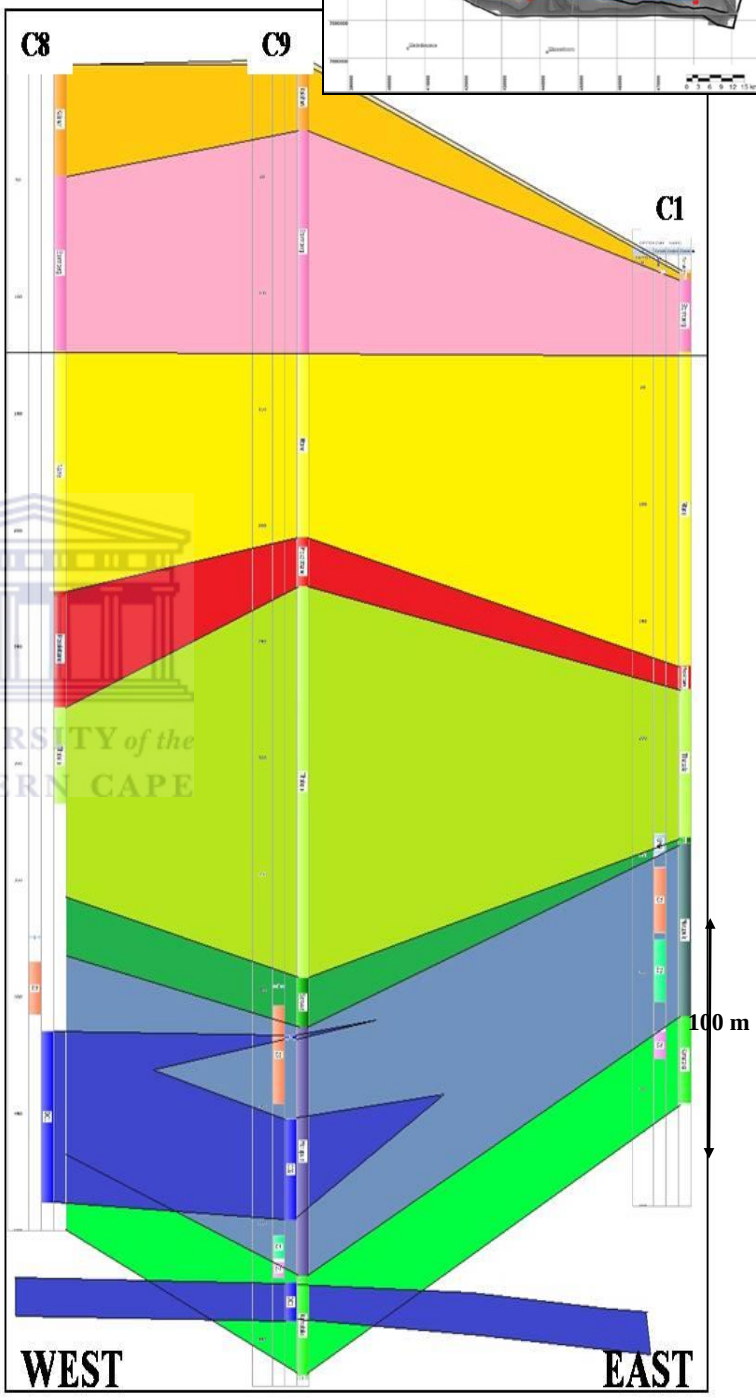

Figure B1.3: An approximate west-east cross section interpreted using the logs provided for boreholes C8, C9 and C1 at the southern end of the study area.

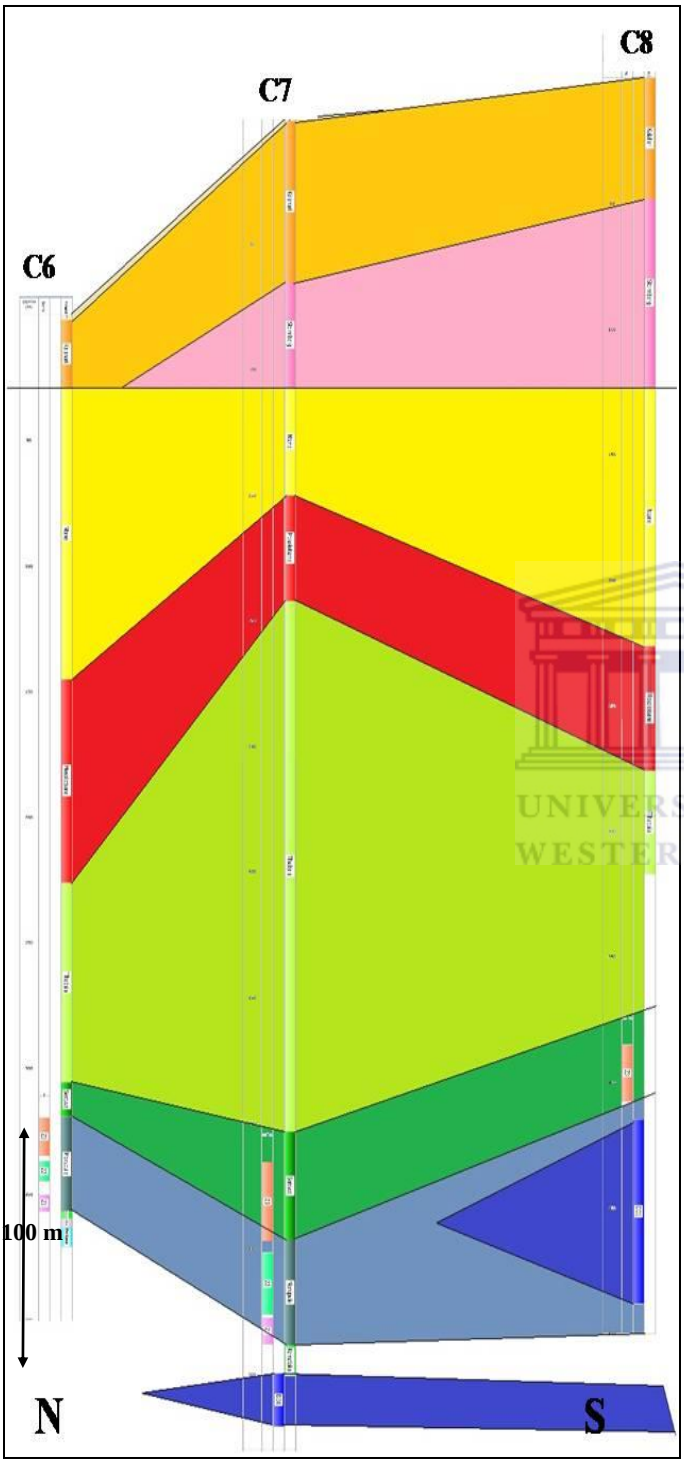

Figure B1.4: An approximate north-south cross section interpreted using logs provided for boreholes C6, C7 and C8, crossing the western part of the study area.

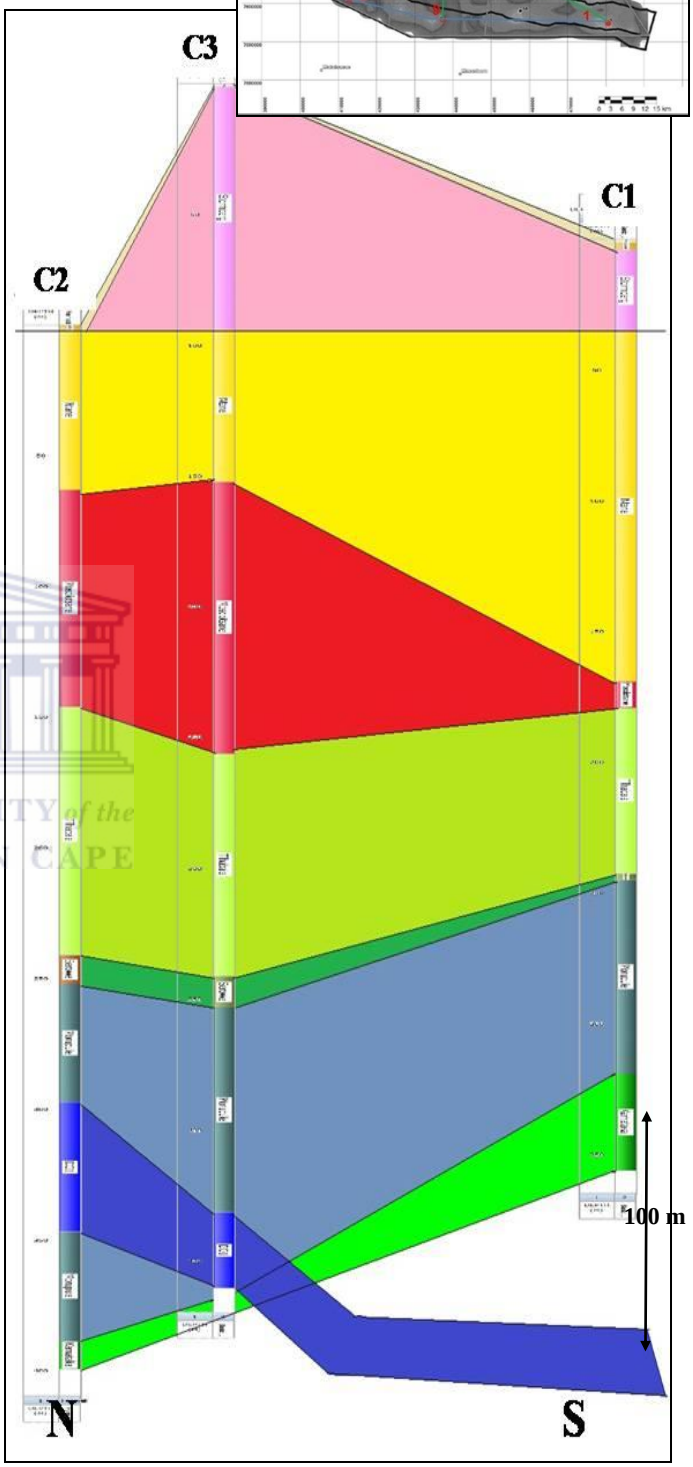

Figure B1.5: An approximate north-south cross section interpreted using logs provided for boreholes C2, C3 and C1 crossing the eastern part of the study area.

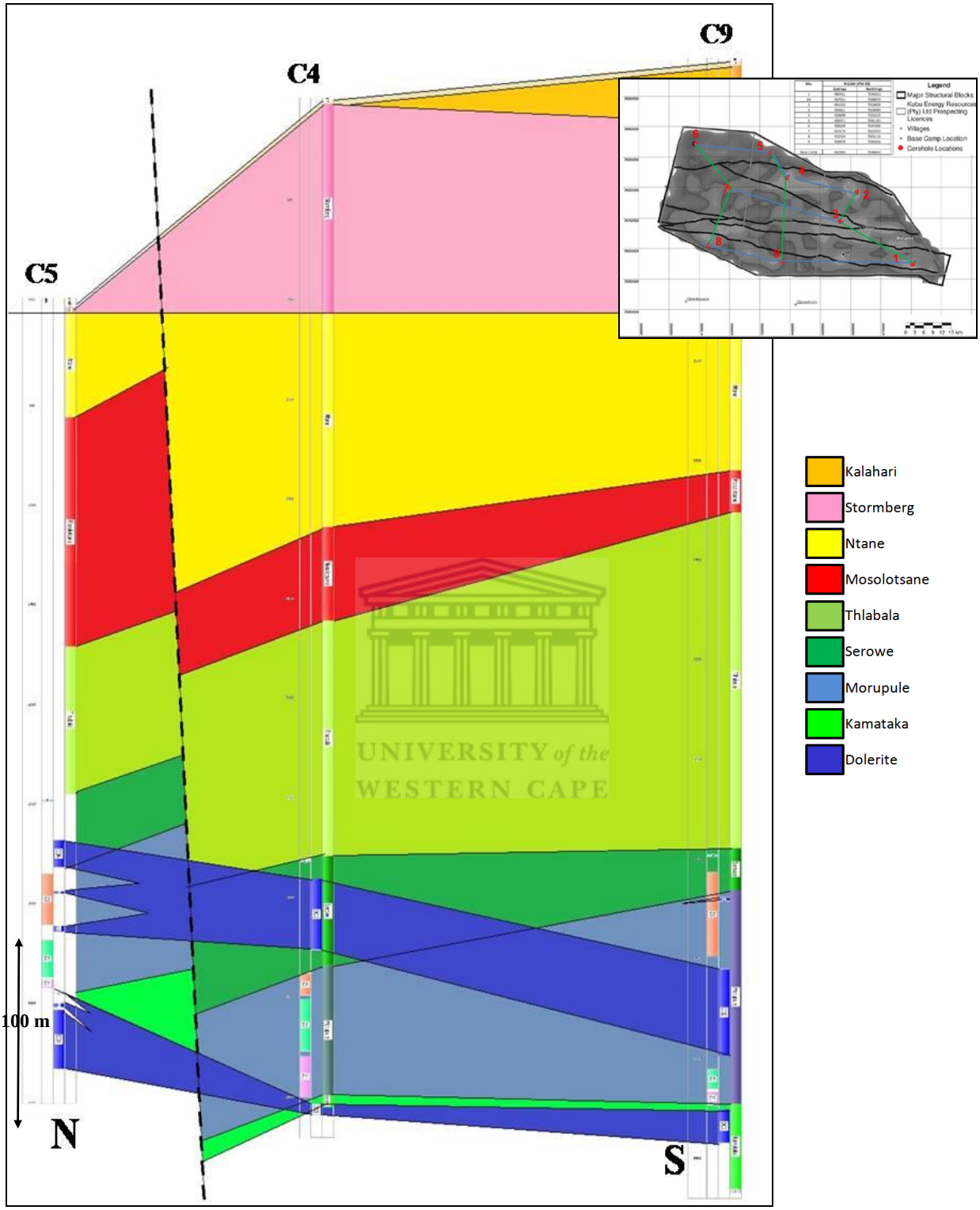

Figure B1.6: An approximate north-south cross section interpreted using logs provided for boreholes C5, C4 and C9 crossing the eastern part of the study area.

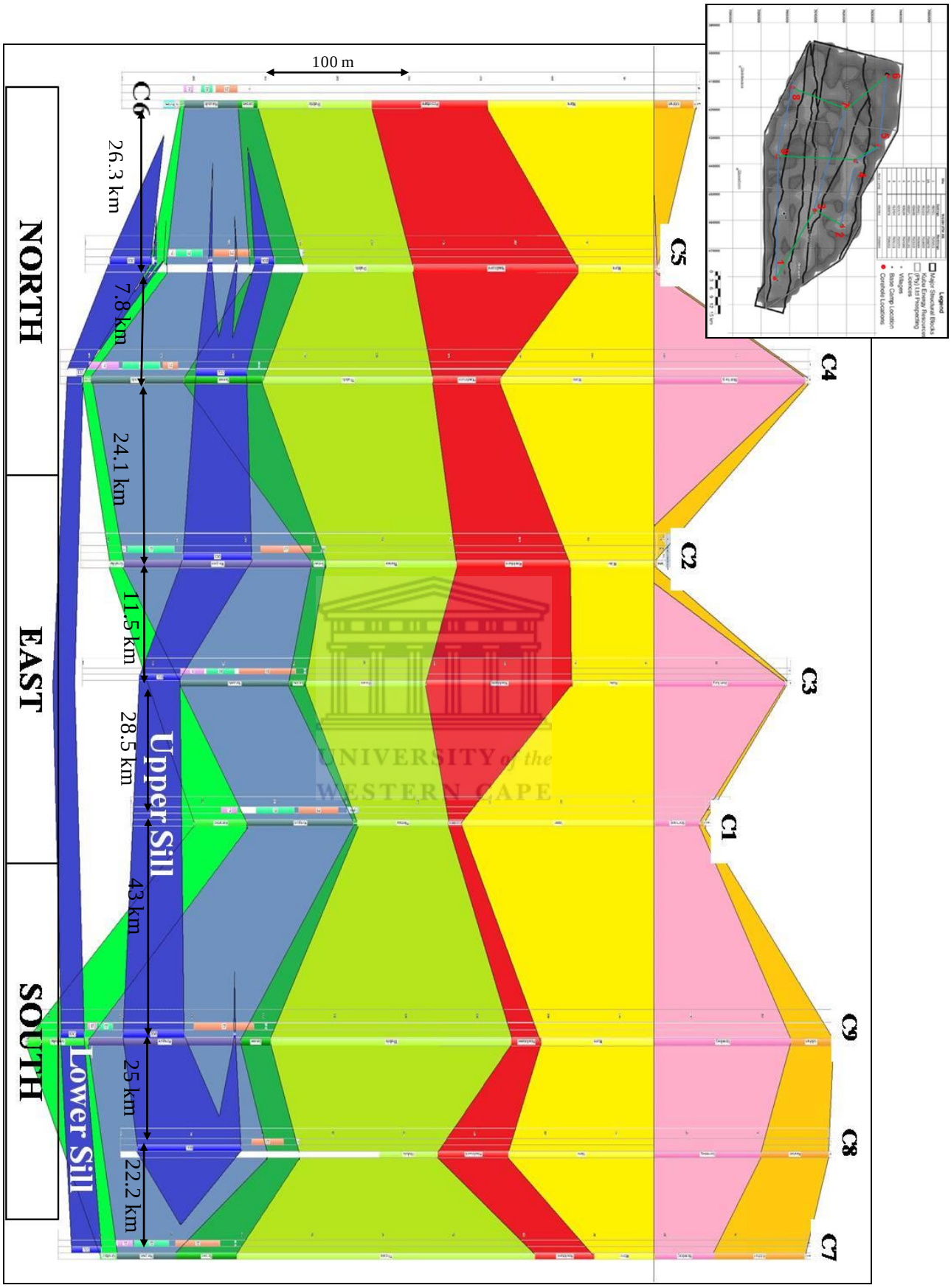

Figure B1.7: A cross section interpreted using all 9 boreholes, circulating in a clockwise direction from the north-west at C6, and ending with C7. This cross section clearly shows the two sills that have been interpreted, i.e. the Upper and the Lower sills, which only tend to consume the country rock at the inclined portions of the sills.

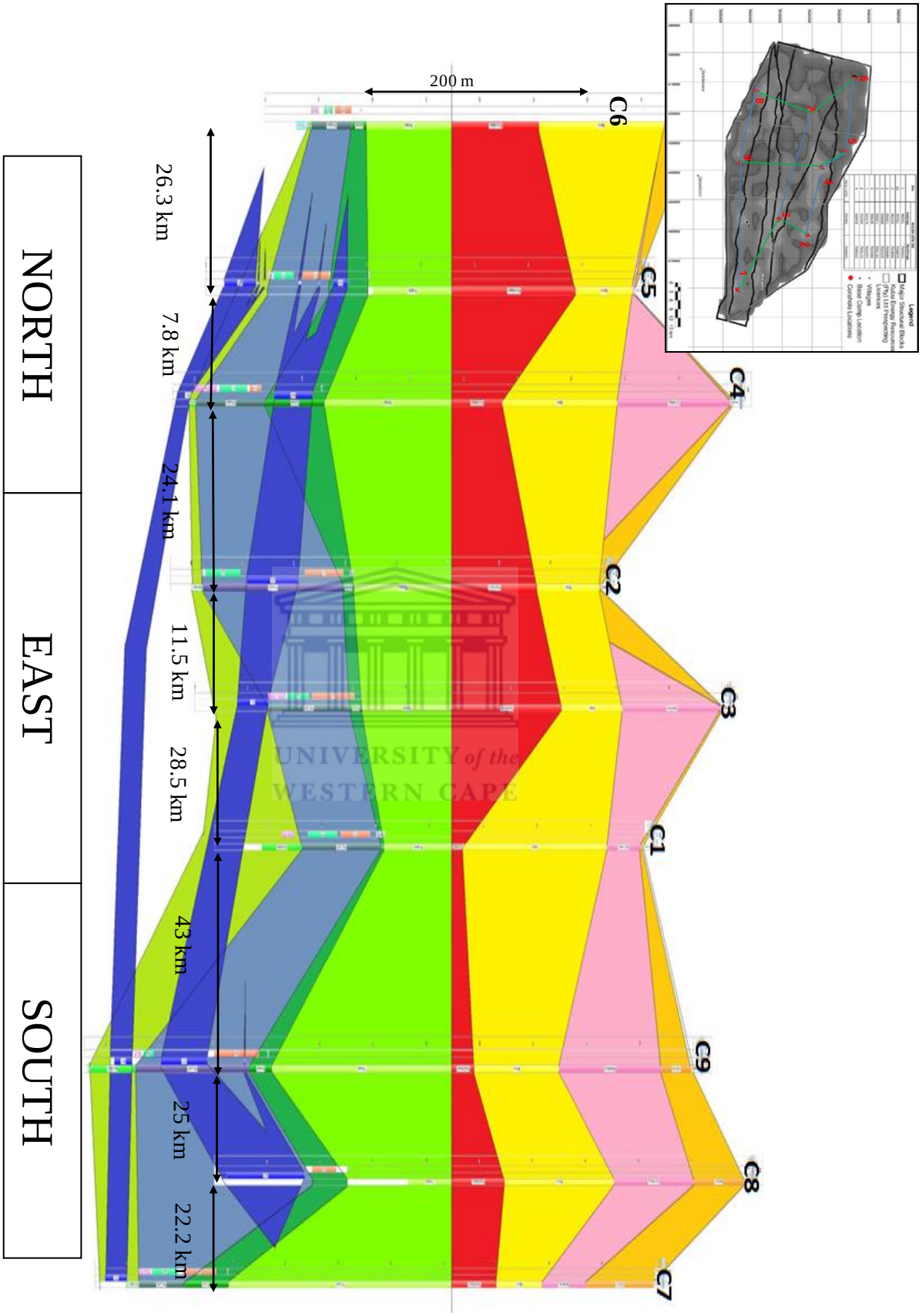

Figure B1.8: A cross section interpreted using all 9 boreholes, circulating in a clockwise direction from the north-west at C6, and ending with C7, using the top of the Tlhabala Formation as the datum. This cross section clearly shows the two sills that have been interpreted, i.e. the Upper and the Lower sills, which only tend to consume the country rock at the inclined portions of the sills.

B2. Cross Sections- Dolerite and Coal Seams

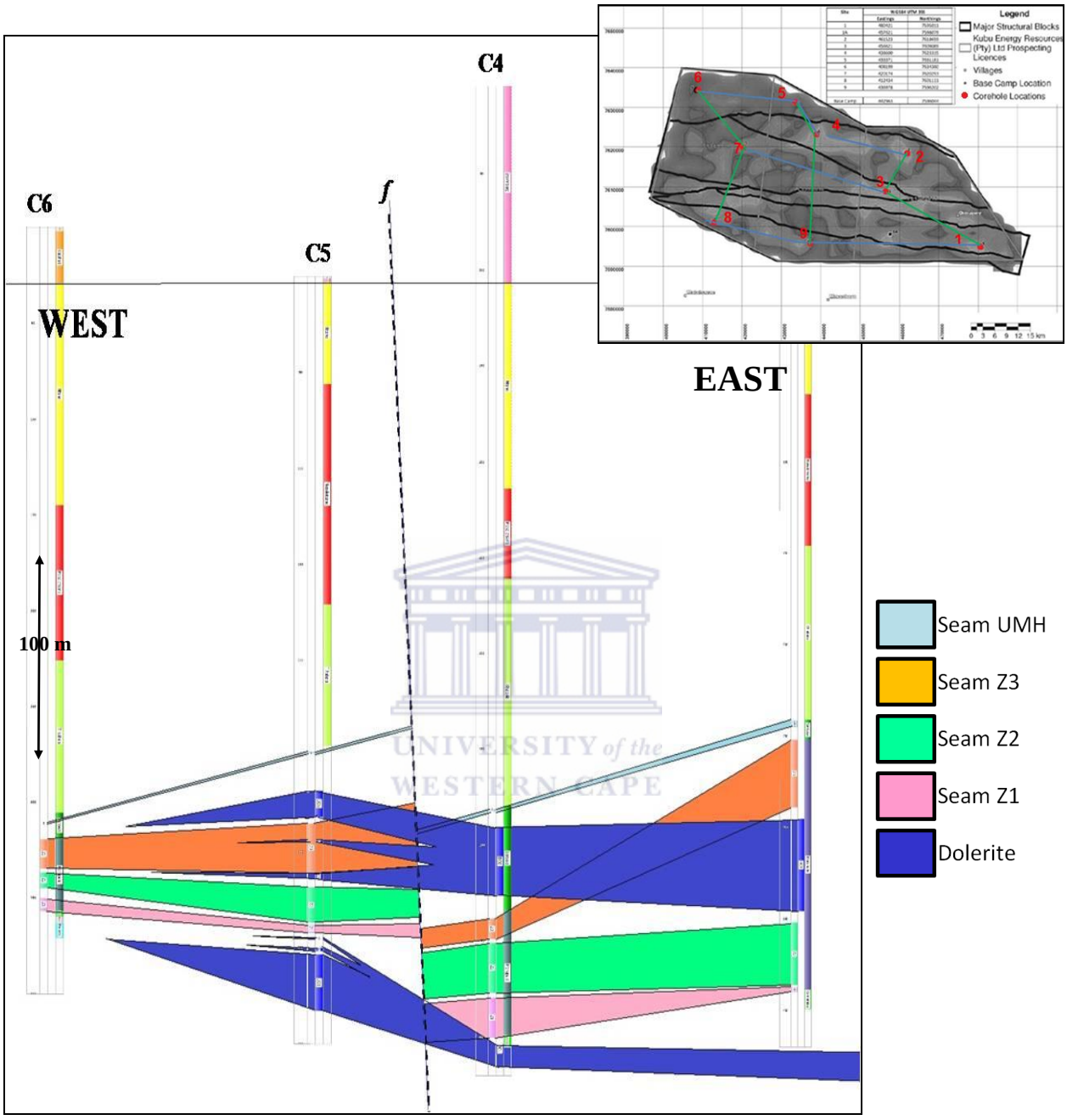

Figure B2.1: An approximate west-east cross section was created using data from boreholes C6, C5, C4 and C2, depicting only the stratigraphic positions of the four seams and the dolerite sills. The legend used in this figure applies to all related figures in Appendix B2.

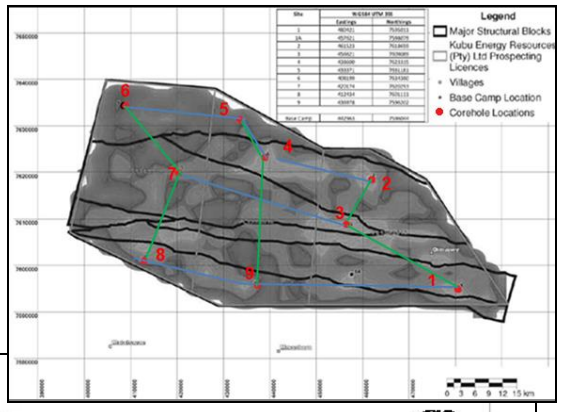

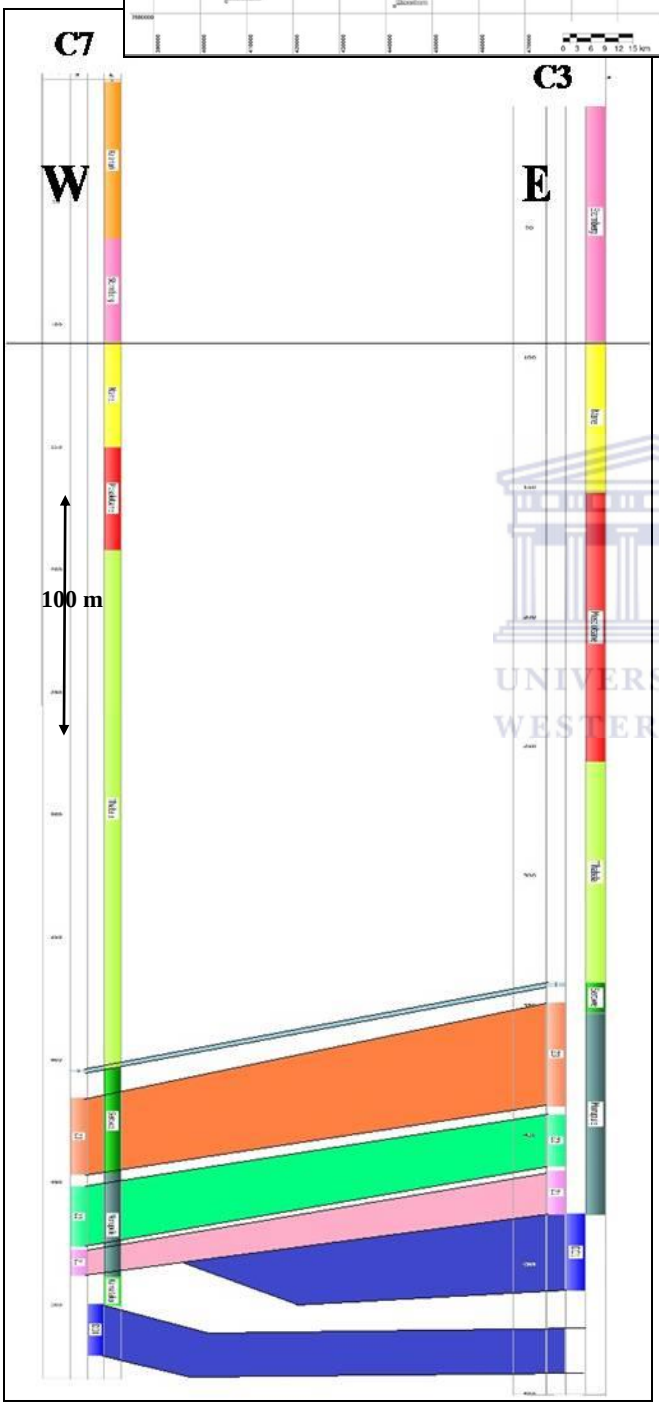

Figure B2.2: An approximate west-east cross section was created using data from boreholes C7 and, C3, depicting only the stratigraphic positions of the four seams and the dolerite sills.

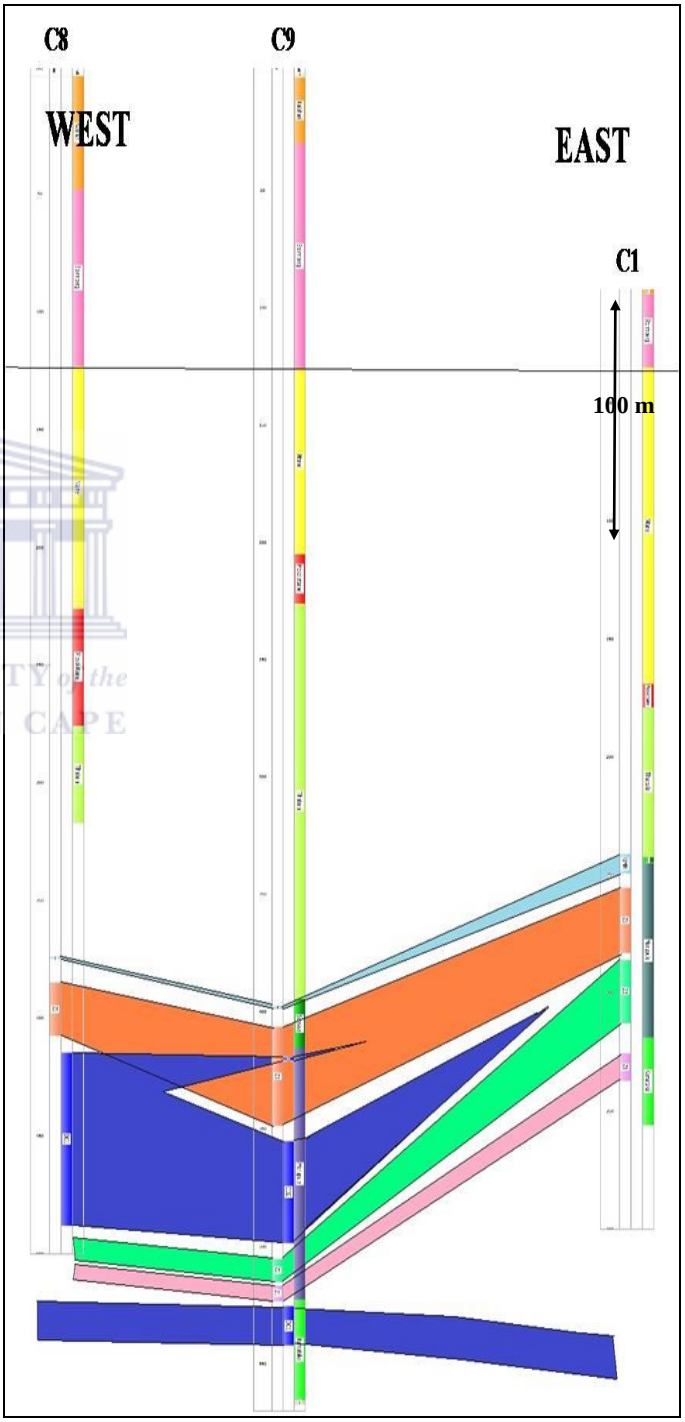

Figure B2.3: An approximate west-east cross section was created using data from boreholes C8, C9, and C1, depicting only the stratigraphic positions of the four seams and the dolerite sills.

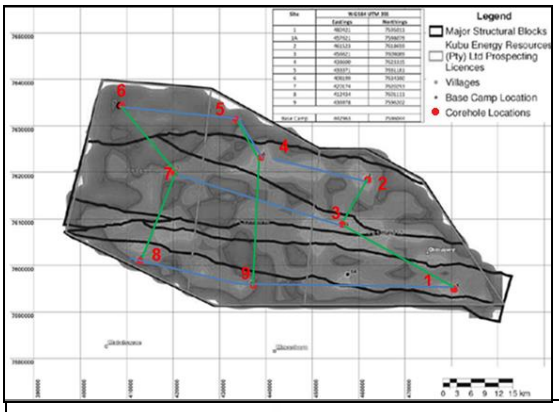

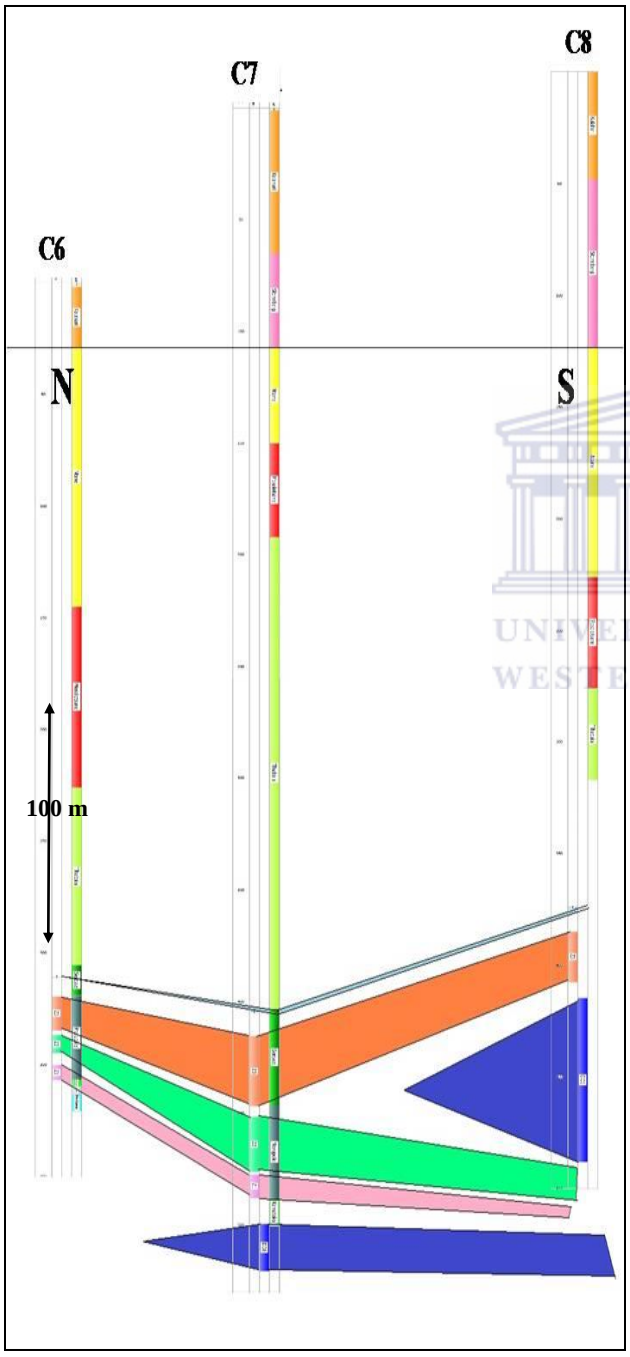

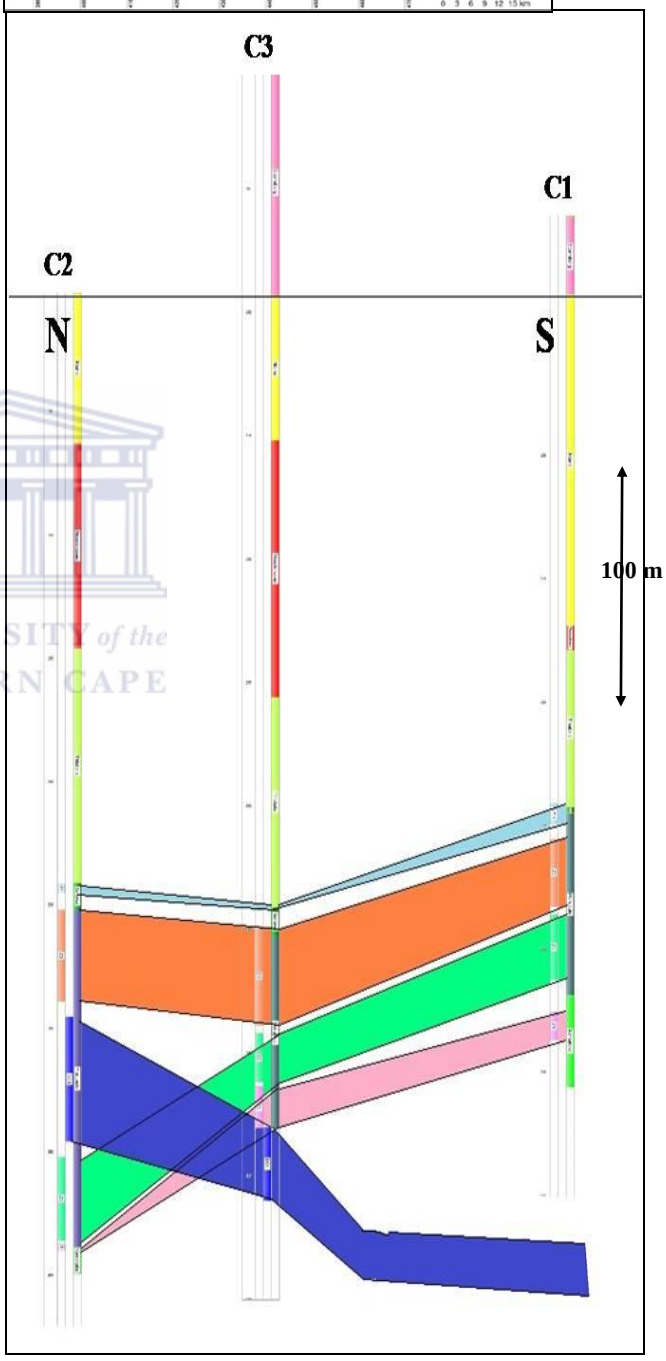

Figure B2.4: An approximate north-south cross section was created using data from boreholes C6, C7, and C8, depicting only the stratigraphic positions of the four seams and the dolerite sills.

Figure B2.5: An approximate north-south cross section was created using data from boreholes C2, C3, and C1, depicting only the stratigraphic positions of the four seams and the dolerite sills.

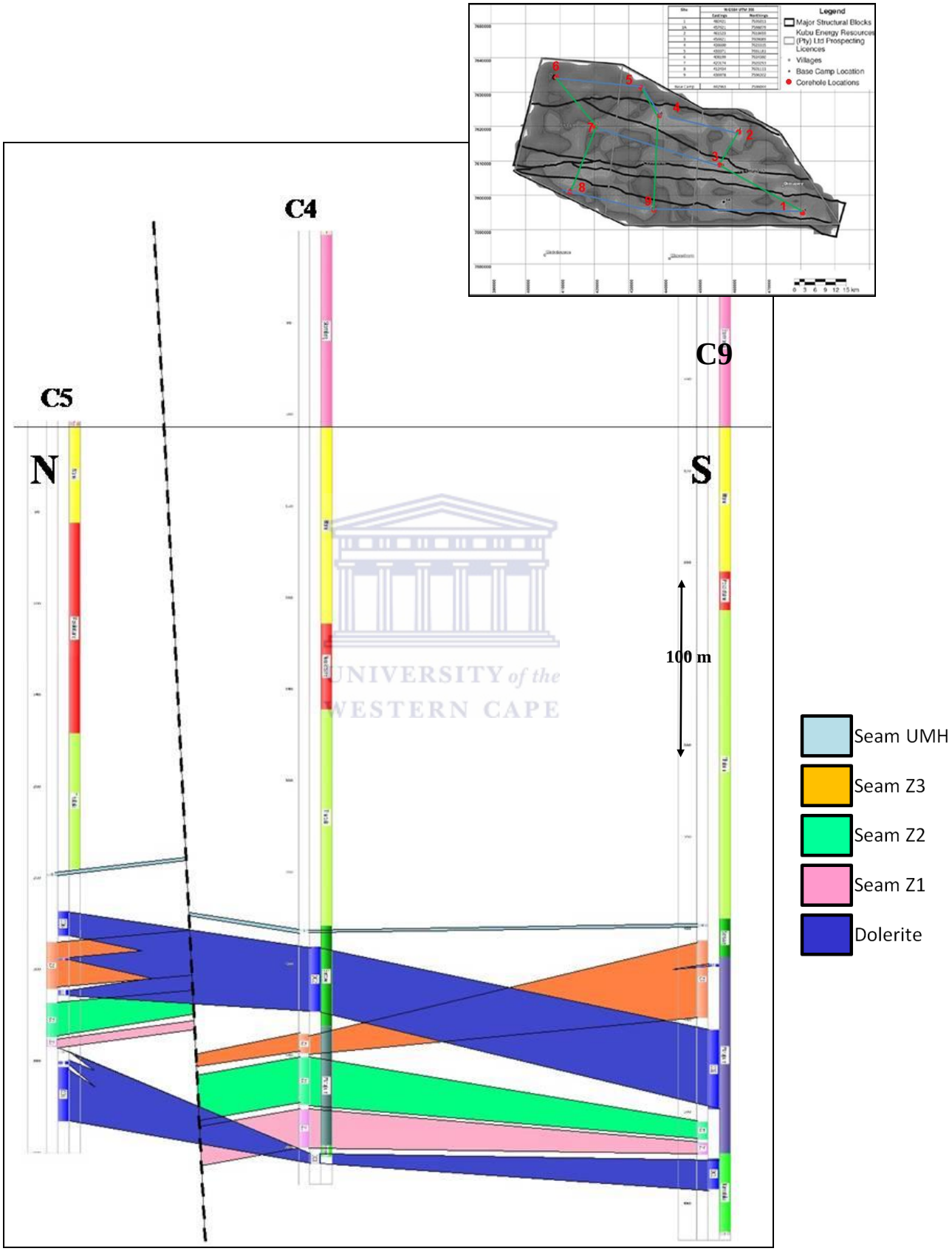

Figure B2.6: An approximate north-south cross section was created using data from boreholes C5, C4, and C9, depicting only the stratigraphic positions of the four seams and the dolerite sills.

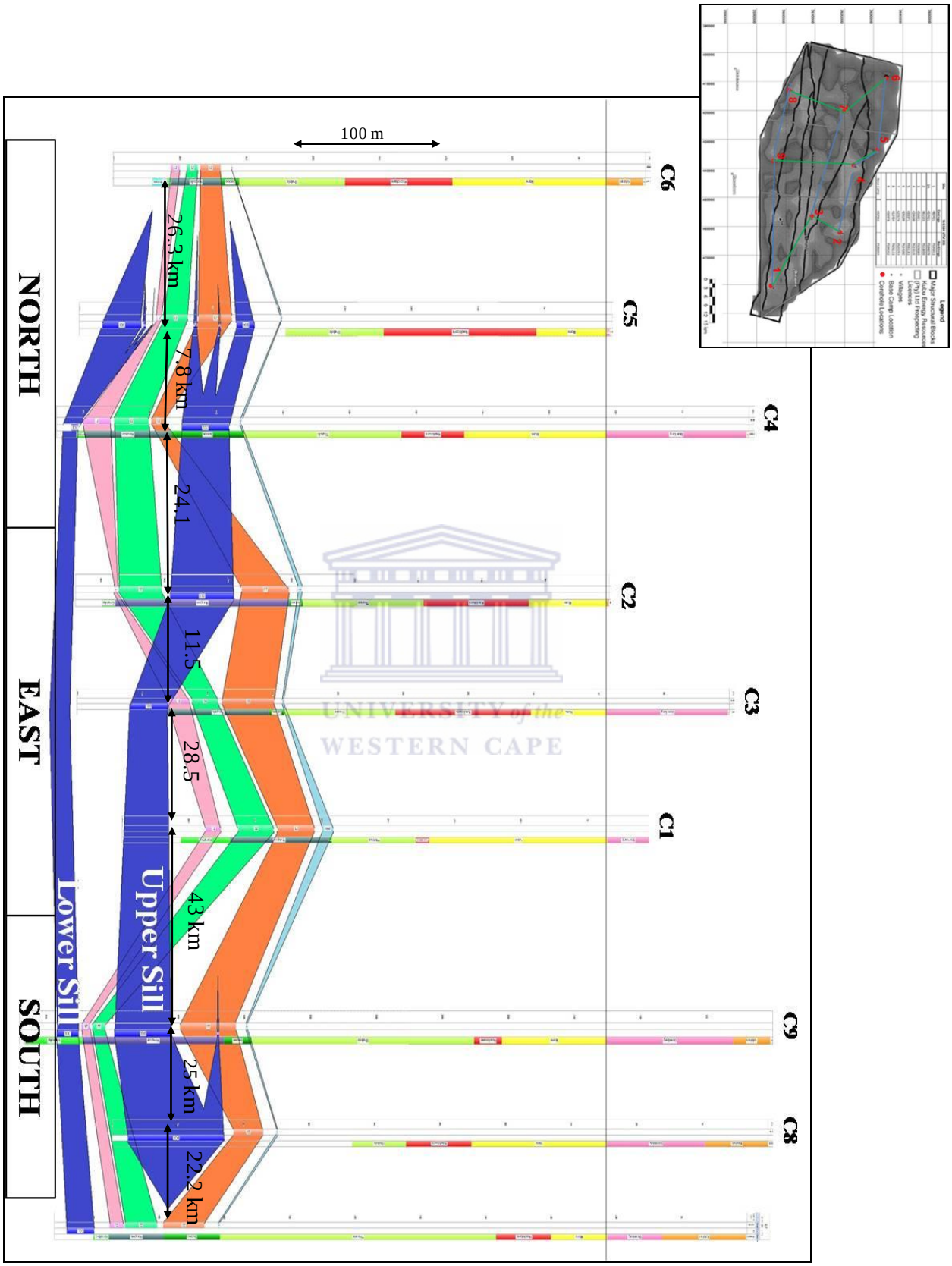

Figure B2.7: A cross section interpreted using all 9 boreholes, proceeding in a clockwise direction from the north-west at C6, and ending with C7. This cross section clearly shows that the two sills that have been interpreted, i.e. the Upper and the Lower sills, have, in general, intruded parallel to the coal seams. In cases where the sills have cut across the seams, as in the region between boreholes C2 and C3, the coal has been consumed. Otherwise, the coal has been displaced, and heat affected in areas where the dolerite is close to, or within the coal seams.

B3. Proximate Data Analysis

Table B3.1: Proximate Analysis done on 8 samples from borehole C1, with the interpreted coal rank. Borehole C1 is used as a control in determining "background" coal rank, as there is no intrusion of dolerite in this locale.

Sample Number	Formation	Top Depth	Bottom Depth	Moisture	Ash	Volatile Matter	Fixed Carbon	Seam	Rank	Comments
		(m)	(m)	(%)	(%)	(%)	(%)			
1G	Serowe	242.4	242.89	5.18	26.92	30.78	37.12	UMH	Subbit	Siderite preset
2G	Morupule	245.82	246.29	5.65	22.11	28.74	43.49	UMH	Subbit	Siderite preset
3G	Morupule	259.05	259.35	5.32	22.51	29.81	42.36	Z3	Subbit	Siderite preset
4G	Morupule	268.38	268.98	5.45	20.23	31.5	42.82	Z3	Subbit	Siderite preset
5G	Morupule	275.24	275.44	5.43	21.04	30.7	42.84	Z3	Subbit	Siderite preset
6G	Morupule	277.3	277.9	4.71	29.99	25.84	39.46	Z3	Subbit	Siderite preset
7G	Morupule	277.9	278.25	4.85	14.62	33.08	47.45	Z3	Subbit	Siderite preset
8G	Morupule	279.96	280.17	5.08	12.37	32.94	49.62	Z3	Subbit	Siderite preset
9G	Morupule	285.66	285.96	4.32	24.93	29.13	41.61	Z2	Subbit	Siderite preset

Table B3.2: Proximate Analysis done on 12 samples from borehole C2, with the interpreted coal rank.

Sample Number	Formation	Top Depth	Bottom Depth	Moisture	Ash	Volatile Matter	Fixed Carbon	Seam	Rank	Comments
		(m)	(m)	(%)	(%)	(%)	(%)			
D01	Serowe	251.25	251.81	3.07	91.07	5.69	0.17	Z3	Non-coal	Mudstone
D02	Morupule	252.12	252.72	4.81	34.96	29.07	31.17	Z3	Subbit	Minor coal
D03	Morupule	257.64	258.25	4.88	26.79	33.52	34.82	Z3	Subbit	
D04	Morupule	262.62	262.94	5.28	18.96	32.10	43.66	Z3	Subbit	
D05	Morupule	263.97	264.30	5.13	25.06	29.76	40.05	Z3	Subbit	Calcite microcleats
D06	Morupule	266.26	266.68	5.14	20.48	30.30	44.08	Z3	Subbit	Siderite Present
D07	Morupule	272.49	273.09	2.69	26.84	27.69	42.78	Z3	Subbit	
D08	Morupule	273.09	273.36	2.32	22.51	28.21	46.96	Z3	Subbit	
D09	Morupule	276.51	276.74	1.45	21.45	16.30	60.81	Z3	Bit	Siderite Present
D10	Morupule	278.16	278.49	1.00	34.77	17.08	47.15	Z3	Bit	Siderite Present
Dolerite at 295.26 - 354.71 m										
D11	Morupule	357.97	358.27	0.76	34.45	18.77	46.02	Z2	Bit	Dense
D12	Morupule	378.71	379.01	5.06	23.67	25.11	46.16	Z2	Subbit	Siderite Present

Table B3.3: Proximate Analysis done on 21 samples from borehole C3, with the interpreted coal rank.

Sample Number	Formation	Top Depth	Bottom Depth	Moisture	Ash	Volatile Matter	Fixed Carbon	Seam	Rank	Comments
		(m)	(m)	(%)	(%)	(%)	(%)			
D001	Morupule	354.40	355.00	6.59	32.68	30.24	30.49	Z3	Subbit	Siderite Present
D003	Morupule	360.07	360.27	7.35	24.60	28.29	39.75	Z3	Subbit	
D004	Morupule	361.37	361.97	3.53	47.15	17.63	31.70	Z3	Meta	Calcite in cleats
D005	Morupule	363.40	364.00	1.67	23.00	27.39	47.93	Z3	Subbit	Siderite Present
D006	Morupule	364.70	365.00	2.10	22.98	29.07	45.84	Z3	Subbit	Siderite Present
D007	Morupule	366.62	367.22	3.36	26.22	27.38	43.04	Z3	Subbit	
D008	Morupule	368.80	369.20	3.75	21.38	31.21	43.66	Z3	Subbit	Siderite Present
D009	Morupule	369.61	370.21	4.06	30.48	26.06	39.39	Z3	Meta	Calcite in cleats
D010	Morupule	370.26	370.58	4.38	22.13	29.37	44.12	Z3	Subbit	
D011	Morupule	372.71	373.31	2.71	23.68	27.32	46.29	Z3	Subbit	
D012	Morupule	373.31	373.78	4.79	19.29	31.56	44.36	Z3	Subbit	Siderite Present
D013	Morupule	374.94	375.54	3.51	45.38	21.51	29.60	Z3	Meta	Calcite in cleats
D014	Morupule	410.45	410.68	4.32	11.79	31.45	52.44	Z2	Bit	
D015	Morupule	414.59	414.81	2.32	53.53	16.94	27.21	Z1	Meta	Dense
D016	Morupule	417.41	417.95	3.60	39.37	17.50	39.54	Z1	Meta	Dense
D017	Morupule	417.95	418.55	3.14	21.62	21.12	54.12	Z1	Bit	Siderite Present
D018	Morupule	420.03	420.63	2.32	35.39	17.39	44.91	Z1	Bit	Siderite Present
D019	Morupule	420.95	421.55	2.05	26.58	17.49	53.88	Z1	Bit	
D020	Morupule	422.82	423.42	1.64	24.81	14.27	59.27	Z1	Bit	Siderite Present
D021	Morupule	428.33	428.90	3.31	32.60	10.20	53.89	Z1	Bit	Siderite Present
Dolerite at: 430.13-459.97 m										

Table B3.4: Proximate Analysis done on 20 samples from borehole C4, with the interpreted coal rank.

Sample Number	Formation	Top Depth	Bottom Depth	Moisture	Ash	Volatile Matter	Fixed Carbon	Seam	Rank	Comments
		(m)	(m)	(%)	(%)	(%)	(%)			
D1	Serowe	380.82	381.53	1.13	42.25	14.25	42.37	UMH	Devol	Calcite in cleats
D2	Serowe	383.11	383.71	2.72	93.73	3.38	0.17	Below UMH	Non-coal	Mudstone
DOLERITE AT: 390.52 - 426.04 M										
D3	Morupule	437.06	437.41	2.27	81.96	4.21	11.57	Z3	Devol	Slightly baked
D4	Morupule	446.44	446.69	1.46	17.95	26.18	54.41	Z3	Subbit	Pyrite cleats
D5	Morupule	447.24	447.44	1.59	17.07	27.69	53.65	Z3	Subbit	Siderite Present
D6	Morupule	450.62	450.82	1.71	33.57	22.74	41.98	Z2	Subbit	
D7	Morupule	450.82	451.40	1.99	18.33	27.46	52.22	Z2	Subbit	Siderite Present
D8	Morupule	451.92	452.17	2.11	19.89	27.12	50.89	Z2	Subbit	
D9	Morupule	457.11	457.31	2.18	12.79	28.73	56.30	Z2	Subbit	Siderite Present
D10	Morupule	459.90	460.02	2.31	13.30	28.53	55.86	Z2	Subbit	
D11	Morupule	464.82	464.98	2.23	15.13	27.40	55.24	Z2	Subbit	Siderite Present
D12	Morupule	465.72	465.97	2.29	7.93	29.42	60.35	Z2	Bit	Calcite in cleats
D13	Morupule	474.89	475.37	1.70	28.91	26.45	42.93	Z2	Subbit	Calcite in cleats
D14	Morupule	478.31	478.67	2.39	13.12	29.26	55.22	Z1	Subbit	
D15	Morupule	478.79	479.34	2.50	17.16	27.13	53.20	Z1	Subbit	Siderite Present
D16	Morupule	483.82	484.13	2.05	23.47	23.73	50.75	Z1	Subbit	
D17	Morupule	486.86	487.36	1.61	11.24	23.05	64.11	Z1	Bit	Siderite Presnet
D18	Morupule	488.31	488.85	1.34	22.55	15.50	60.61	Z1	Bit	Siderite Presnet
D19	Morupule	490.40	490.64	1.06	13.75	11.27	73.92	Z1	Anthracite	Vitrinite visible
D20	Morupule	496.44	496.54	2.49	19.00	6.34	72.17	Z1	Anthracite	Vitrinite visible
DOLERITE AT: 503.6-508.74 m										

Table B3.5: Proximate Analysis done on 12 samples from borehole C5, with the interpreted coal rank.

Sample Number	Formation	Top Depth	Bottom Depth	Moisture	Ash	Volatile Matter	Fixed Carbon	Seam	Rank	Comment
		(m)	(m)	(%)	(%)	(%)	(%)			
1	Serowe	247.77	248.50	1.85	24.56	22.65	50.94	UMH	Bit	Calcite microveins
Dolerite at: 267.94 - 281.77 m										
2	Serowe	283.00	283.25	2.43	48.50	6.57	42.50	Z3	Devol	
Dolerite at 293.84 - 295.05 m										
Dolerite at: 311.20 - 314.11 m										
3	Morupule	322.33	322.74	2.76	18.58	29.62	49.03	Z2	Subbit	Calcite in cleats
4	Morupule	322.74	323.34	2.48	20.25	27.87	49.40	Z2	Subbit	Calcite in cleats
5	Morupule	325.77	328.46	2.21	31.35	23.61	42.83	Z2	Subbit	Calcite in cleats
6	Morupule	331.74	332.70	2.10	34.86	22.15	40.90	Z2	Subbit	Calcite in cleats
7	Morupule	333.79	334.39	1.97	32.93	20.04	45.06	Z2	Subbit	Calcite in cleats
8	Morupule	334.39	334.69	1.86	31.63	20.67	45.84	Z2	Subbit	Calcite in cleats
9	Morupule	335.26	336.29	1.37	17.26	22.11	59.25	Z2	Bit	Siderite
10	Morupule	338.15	338.62	1.10	28.23	13.94	56.73	Z1	Bit	Rare calcite microve
11	Morupule	344.10	345.14	2.27	57.05	8.38	32.30	Z1	Devol	Slightly baked
Dolerite at: 344.97 -345.07 m										
Dolerite at: 350.02-351.88 m										
12	Morupule	353.00	353.27	1.98	62.14	5.38	30.49	Z1	Devol	Highly baked
Dolerite at: 353.97 - 382.74 m										

Table B3.6: Proximate Analysis done on 16 samples from borehole C6, with the interpreted coal rank. Borehole 61 is used as a control in determining "background" coal rank, as there is no intrusion of dolerite in this locale.

Sample Number	Formation	Top Depth	Bottom Depth	Moisture	Ash	Volatile Matter	Fixed Carbon	Seam	Rank	Comments
		(m)	(m)	(%)	(%)	(%)	(%)			
D001	Morupule	319.04	319.59	5.16	47.02	21.54	26.29	Z3	Meta	Fractured
D002	Morupule	319.59	320.19	5.99	42.21	23.38	28.41	Z3	Meta	Calcite veins and cleats
D003	Morupule	320.19	320.79	6.13	12.33	36.95	44.59	Z3	Subbit	Calcite in cleats
D004	Morupule	320.93	321.23	5.94	15.97	35.80	42.29	Z3	Subbit	Siderite Present
D005	Morupule	324.00	324.57	3.02	54.44	19.76	22.79	Z3	Meta	Calcite veins and cleats
D006	Morupule	324.80	325.40	4.42	16.26	35.11	44.21	Z3	Subbit	
D007	Morupule	326.04	326.64	5.43	27.89	27.91	38.78	Z3	Subbit	Siderite Present
D008	Morupule	328.84	329.40	5.27	16.07	34.62	44.04	Z3	Subbit	Calcite veins and cleats
D009	Morupule	329.40	330.00	3.89	23.76	33.72	38.63	Z3	Subbit	
D010	Morupule	333.47	334.07	5.01	18.26	33.31	43.42	Z3	Subbit	Siderite Present
D011	Morupule	338.86	339.45	3.57	35.85	28.42	32.15	Z2	Subbit	
D012	Morupule	339.45	340.05	4.68	22.98	32.23	40.11	Z2	Subbit	
D013	Morupule	340.05	340.64	4.98	13.60	32.00	49.41	Z2	Subbit	Siderite Present
D014	Morupule	340.64	341.09	4.00	29.79	28.54	37.68	Z2	Subbit	Calcite in cleats
D015	Morupule	354.69	354.98	3.44	48.51	15.06	32.99	Z1	Meta	Highly fractured
D016	Morupule	355.50	355.99	2.42	63.10	13.18	21.30	Z1	Non-coal	Mudstone

Table B3.7: Proximate Analysis done on 25 samples from borehole C7, with the interpreted coal rank.

Sample Number	Formation	Top Depth	Bottom Depth	Moisture	Ash	Volatile Matter	Fixed Carbon	Seam	Rank	Comments
		(m)	(m)	(%)	(%)	(%)	(%)			
1G	Serowe	403.47	403.83	6.21	43.71	25.56	24.52		Meta	Highly fractured
2G	Serowe	403.83	404.43	6.36	29.78	32.85	31.01	UMH	Subbit	Calcite in fractures
3G	Serowe	415.22	415.82	5.15	39.33	23.80	31.73	Z3	Devol	Siderite is common
4G	Serowe	416.70	417.30	5.89	31.74	25.30	37.08	Z3	Subbit	Abundand siderite
5G	Serowe	417.30	417.90	6.48	15.09	32.00	46.43	Z3	Subbit	Abundand siderite
6G	Serowe	418.04	418.47	5.42	21.52	29.44	43.63	Z3	Subbit	Abundand siderite
7G	Serowe	418.87	419.25	4.09	39.78	31.26	24.86	Z3	Non-coal	Mudstone and coal
8G	Serowe	423.08	423.68	4.77	14.42	33.49	47.32	Z3	Subbit	Siderite present
9G	Serowe	423.68	424.28	5.05	15.23	33.64	46.08	Z3	Subbit	Siderite present
10G	Serowe	428.23	428.72	3.91	31.31	32.09	32.70	Z3	Subbit	Siderite present
11G	Serowe	432.36	432.96	4.78	13.91	33.51	47.81	Z3	Subbit	Siderite present
12G	Serowe	432.96	433.56	4.09	17.17	31.58	47.17	Z3	Subbit	Siderite present
13G	Serowe	433.92	434.52	3.79	22.26	30.01	43.94	Z3	Subbit	Siderite present
14G	Serowe	438.75	439.35	3.67	20.70	30.39	45.24	Z3	Subbit	Siderite present
15G	Serowe	439.35	439.95	3.84	13.30	35.68	47.18	Z3	Subbit	Siderite present
16G	Serowe	439.95	440.55	3.52	22.65	28.88	44.95	Z3	Subbit	Siderite present
17G	Morupule	451.38	451.75	2.89	29.19	34.14	33.78	Z2	Subbit	Abundand siderite
18G	Morupule	456.37	456.93	3.65	19.86	32.31	44.19	Z2	Subbit	Siderite present
19G	Morupule	456.93	457.50	3.11	27.09	34.23	35.58	Z2	Subbit	Siderite present
20G	Morupule	460.24	460.70	3.58	23.72	31.11	41.59	Z2	Subbit	Siderite present
21G	Morupule	462.86	463.14	3.72	12.91	32.05	51.33	Z2	Bit	Siderite present
22G	Morupule	469.69	470.29	2.65	37.57	31.34	28.44	Z2	Devol	Clean fractures
23G	Morupule	473.55	474.15	3.44	36.34	17.73	42.50	Z2	Devol	Clean fractures
24G	Morupule	481.69	482.29	1.61	25.56	16.50	56.33	Z1	Bit	Clean fractures
25G	Morupule	485.62	486.22	1.30	22.10	9.42	67.18	Z1	Devol	Calcite in fractures
Dolerite at 499.54 - 520.79 m										

Table B3.8: Proximate Analysis done on 13 samples from borehole C8, with the interpreted coal rank.

Sample Number	Formation	Top Depth	Bottom Depth	Moisture	Ash	Volatile Matter	Fixed Carbon	Seam	Rank	Comment
		(m)	(m)	(%)	(%)	(%)	(%)			
D1	Serowe	369.88	370.48	3.51	35.18	28.52	32.79	UMH	Meta	Calcite in cleats
D2	Serowe	370.48	370.86	3.36	29.07	33.58	33.99	UMH	Subbit	
D3	Serowe	381.07	381.37	3.44	30.62	29.30	36.64	Z3	Subbit	
D4	Serowe	383.02	383.62	3.01	38.98	23.50	34.51	Z3	Meta	Calcite microveins
D5	Serowe	383.62	384.22	3.15	22.79	27.91	46.15	Z3	Subbit	
D6	Serowe	384.25	384.88	3.08	37.68	23.29	35.96	Z3	Meta	Calcite in cleats
D7	Serowe	384.88	385.48	2.59	36.60	22.73	38.08	Z3	Non-coal	Mudstone
D8	Serowe	385.48	386.08	2.83	45.62	18.55	32.99	Z3	Meta	Calcite in cleats
D9	Serowe	386.08	386.68	2.70	17.28	28.88	51.15	Z3	Bit	Calcite in cleats
D10	Serowe	386.68	387.28	2.93	32.92	23.91	40.24	Z3	Subbit	
D11	Serowe	387.28	387.63	2.25	30.64	23.67	43.44	Z3	Subbit	
D12	Serowe	387.88	388.48	2.66	46.71	16.99	33.64	Z3	Meta	
D13	Serowe	388.48	388.88	1.81	25.95	23.54	48.70	Z3	Subbit	
Dolerite at 414.51 - 487.94 m										

Table B3.9: Proximate Analysis done on 31 samples from borehole C9, with the interpreted coal rank.

Sample Number	Formation	Top Depth	Bottom Depth	Moisture	Ash	Volatile Matter	Fixed Carbon	Seam	Rank	Comments
		(m)	(m)	(%)	(%)	(%)	(%)			
AB1	Serowe	397.85	398.45	3.63	30.82	28.89	36.66	UMH	Subbit	
AB2	Serowe	405.7	406.3	3.81	39.94	22.04	34.21	Z3	Meta	Calcite in cleats
AB3	Serowe	406.39	406.99	3.66	43.95	21.68	30.71	Z3	Devol	Baked at the bottom
AB4	Serowe	410.52	411.12	3.14	32.18	23.53	41.14	Z3	Devol	Baked
AB5	Serowe	416.42	417.02	2.03	54.51	9.32	34.14	Z3	Devol	vitrinite visible
AB6	Serowe	417.02	417.62	1.61	46.51	7.73	44.15	Z3	Devol	
AB7	Serowe	417.9	418.5	1.58	40.68	8.04	49.69	Z3	Devol	
Dol at: 419.19 - 420.8 m										
AB8	Serowe	420.8	421.4	1.52	58.09	6.03	34.37	Z3	Devol	Baked
AB9	Serowe	421.8	422.4	1.53	43.04	11.29	44.14	Z3	Devol	Baked
AB10	Serowe	422.44	423.04	1.32	57.88	6.59	34.21	Z3	Non-coal	Mudstone
AB11	Serowe	424.07	424.67	2.32	53.94	12.29	31.45	Z3	Non-coal	Mudstone
AB12	Serowe	424.92	425.52	2.22	46.83	16.12	34.84	Z3	Non-coal	Mudstone
AB13	Serowe	427	427.6	2.32	15.82	25.07	56.8	Z3	Bit	
AB14	Serowe	428.75	429.35	2.61	43.16	17.88	36.36	Z3	Non-coal	Mudstone
AB15	Serowe	429.8	430.4	2.68	37.3	19.3	40.72	Z3	Subbit	Calcite
AB16	Serowe	430.96	431.56	2.41	29.15	21.8	46.64	Z3	Subbit	Siderite
AB17	Serowe	439.48	439.78	2.2	40.23	17.51	40.06	Z3	Meta	Calcite in cleats
A18	Serowe	444.21	444.81	1.91	40.61	15.51	41.97	Z3	Meta	Calcite in cleats
AB19	Serowe	446.12	446.72	1.98	72.51	9.38	16.13	Z3	non-coal	Mudstone
AB20	Serowe	446.72	447.32	1.89	52.37	10.01	35.73	Z3	non-coal	Mudstone
AB21	Serowe	450.22	450.82	2.01	84.64	7.02	6.33	Z2	non-coal	Mudstone
AB22	Serowe	451.02	451.62	2.13	72.17	6.13	19.58	Z2	non-coal	Mudstone
AB23	Serowe	452.03	452.63	2.36	85.75	7.18	4.72	Z2	non-coal	Mudstone
AB24	Serowe	453.78	454.38	3.29	76.67	5.84	14.2	Z2	non-coal	Baked Mudstone
AB25	Serowe	454.4	455	2.75	67.32	7.13	22.8	Z2	non-coal	Baked Mudstone
DOL at: 455 - 498.55 m										
AB26	Morupule	502.9	503.5	2.74	58.25	7.86	31.14	Z2	Devol	Baked coal
AB27	Morupule	504	504.6	3.28	76.77	5.81	14.13	Z2	non-coal	Mudstone
AB28	Morupule	504.6	505.2	3.4	74.27	5.95	16.38	Z2	non-coal	Mudstone
AB29	Morupule	512.12	512.72	3.55	60.22	6.74	29.49	Z2	non-coal	Mudstone
AB30	Morupule	519.98	520.58	2.84	33.09	17.83	46.23	Z1	Subbit	
AB31	Morupule	520.86	521.46	2.07	26.64	17.82	53.46	Z1	Bit	
DOL at: 525.25 - 542.11 m										